Theoretical predictions of the oscillating mechanism in cyanobacterial circadian rhythms

Hisako IMAMURA

DOCTOR OF
PHILOSOPHY

Department of Basic Biology
School of Life Science
The Graduate University for Advanced Studies

2007

Table of Contents

Chapter I:
General Introduction

All organisms on earth are exposed to the fluctuating environment of the day-night cycle. As a result, organisms including prokaryotes, plants and animals have evolved mechanisms to adjust their physiology, metabolism, and behavior to such environmental changes. Such mechanisms are widely known as circadian clocks (*circa* = about, *dies* = a day) and involve endogenous oscillations with a period of about 24 h. The clock allows organisms to anticipate daily changes and to prepare for the right activity at an appropriate timing. This mechanism is energetically economical and remarkably advantageous for reproductive fitness and survival in nature (Lakin-Thomas and Brody, 2004; Young and Kay, 2001). Acquisition and development of the circadian clock has been much focused on as an adaptive strategy in the course of evolution. Moreover, circadian rhythms are fundamental to photoperiodism events involving seasonal breeding, hibernation, and flowering regulation.

In mammals, diverse vital functions such as sleeping, feeding, cardiac rate, blood pressure, hepatic function, body temperature, and hormonal production exhibit circadian rhythms (Foster and Kreitzman, 2004). Especially for humans, the maintenance of the sleep-wake cycle is necessary to organize one's social life. The occurrences of health hazards such as insomnia or depression arising from sleep disorders have increased in recent years (Foster and Kreitzman, 2004). An accurate internal clock is thus crucial in the struggle for survival in both nature and civilized society.

The circadian clock that controls diverse and sophisticated phenomena at an individual level is cell autonomous, and persists in the absence of environmental cues. Molecular biological studies have revealed that the essential mechanisms for these endogenous and self-sustaining rhythms are cyclic expressions of the responsible genes, so called clock genes. In mammals, the rhythms in each neuron are synchronized and amplified in the suprachiasmatic nucleus where

photic entrainment occurs. This master clock regulates endocrine output and orchestrates clocks in peripheral tissues. From the perspective of systems biology, the hierarchical structure of the circadian clock appears an excellent model of the complex systems that result from intercellular interactions.

Taken together, the mechanism of circadian rhythms is an interdisciplinary subject covering physiology, neuroscience, and cellular, molecular, and systems biology. Indeed, its elucidation is driven by the growing social and medical demands.

Another approach for circadian research that can be seen as indispensable is a mathematical one. The earliest model predicting oscillations due to transcriptional negative feedback was proposed by Goodwin (Goodwin, 1965) at a time when the role of such a regulatory mechanism in the origin of circadian rhythms was not yet known. One of the best characterized interactions of clock genes is that of *Drosophila*, in which the PER/TIM complex indirectly represses transcriptions of *period* and *timeless*, by binding to the transcription factor CLOCK protein (Dunlap, 1999). This transcriptional feedback mechanism, together with phosphorylation of clock proteins, is remarkably well conserved in other animals, such as *Neurospora*, *Arabidopsis* and mouse, and seems to be a general requirement for self sustaining circadian oscillations (Hardin, 2006; Wijnen and Young, 2006; Young and Kay, 2001). Theoretical studies have confirmed the importance of delayed negative feedback for rhythm generation (Goldbeter, 1995). This portrayal of the transcription-translation feedback oscillator (TTO) has indeed been a dogma in respect to circadian rhythm (Appendix I).

As well as circadian rhythms, mathematical studies have also provided insights into the properties of other biological rhythms (Goldbeter, 2002). The first such application was in ecology to study oscillations resulting from

interactions between prey and predators (Murray, 1989b). In cellular physiology, Hodgkin and Huxley developed a model of neural rhythms, which remains at the core of most models related to oscillating membrane potentials (Keener and Sneyd, 1998). Structural perspectives obtained from mathematical analyses often relate to the general conditions for oscillations and can be applied to other rhythmic phenomena. Investigations of biological rhythms often utilize the store of existing knowledge. Recently, tasks to which mathematical approaches have been applied are increasing. Because of the substantial progress that has been made in molecular biology, the picture of the interacting networks of proteins, RNA and genes that go to make up a biological function is an increasingly exhaustive one. In circadian studies, investigations at the molecular level have revealed multiple coupling networks of feedback loops for which the total behavior is difficult to comprehend (Glossop *et al.*, 1999). In view of the complexity of the associated processes, mathematical analysis and numerical simulations are needed to present a global description of how the network might be organized. As well, these investigations reveal possibilities of being able to suggest novel components or missing connections in the regulatory networks. It is expected that theoretical predictions and experimental identifications will combine to give a clearer understanding of the global mechanism involved, and in return improve mathematical modeling and experimental designs.

Cyanobacteria are thought to have been the first oxygen-evolving photosynthetic organisms on Earth (Ditty *et al.*, 2003). Oxygenic photosynthesis originating in these bacteria is thought to be responsible for changing the prehistoric environment to an oxygen-enriched atmosphere and for creating the ozone layer (Ditty *et al.*, 2003). Photosynthesis in cyanobacteria is repressed rhythmically by the clock, saving unnecessary energy expenditure at night. This

is an adaptive mechanism, as co-culture competition experiments have demonstrated that there is a selective advantage for cells those internal timekeepers are in tune with the rhythms of their environment (Woelfle *et al.*, 2004). The discovery of cyanobacterial circadian rhythms overturned past dogmas that held: (1) that organisms with a cell division time of less than 24 h could not sustain a circadian rhythm, and (2) that prokaryotes could not sustain rhythmicity because cellular complexity and organelles, particularly a membrane-bound nucleus, were required (Kondo *et al.*, 1997; Mori *et al.*, 1996). Moreover, the existence of prokaryotic circadian rhythms enabled simple investigations and observations of the circadian mechanism. For this purpose, *Synechococcus elongatus* PCC 7942, a genetically tractable strain, was developed as a model organism where circadian rhythms could be visualized by introducing the luciferase reporter system (Kondo *et al.*, 1993).

In *S. elongatus*, the clock protein KaiC regulates genome-wide expressions including that of *kai* genes in continuous light conditions (Kondo *et al.*, 1997; Nakahira *et al.*, 2004). This transcriptional autoregulation is consistent with the TTO model (Ishiura *et al.*, 1998). Phosphorylation of the clock protein is proposed to play a critical role in transcriptional regulation in the cyanobacterial clock system (Iwasaki *et al.*, 2002; Nishiwaki *et al.*, 2004; Xu *et al.*, 2004). In Chapter II: Transcriptional Autoregulation by KaiC, I predict how KaiC regulates transcriptional activity depending on its phosphorylated state. I give a theoretical insight into how this mechanism contributes to robust oscillations. The study has been published as “Transcriptional autoregulation by phosphorylated and non-phosphorylated KaiC in cyanobacterial circadian rhythms” in the *Journal of Theoretical Biology*.

The finding of the circadian cycling of KaiC phosphorylation without

transcription has broken the last dogma regarding the TTO (Nakajima *et al.*, 2005; Tomita *et al.*, 2005). In addition to its chronobiological importance, the non-TTO Kai oscillator is an inspiring theme for mathematical research in terms of oscillations derived from purely biochemical interaction in a closed system. This minimal system seen in cyanobacteria cannot be reproduced by the two-variable framework that I used in Chapter II, which focused on the TTO mechanism. Here, I focus on the significance of the variety of KaiC states. I speculate that some processes among complex formations and possible variations of KaiC phosphorylation would be required for rhythm generation. Indeed, theoretical study has demonstrated that a network comprised of a small number of elements cannot generate oscillations, and that multiple reaction steps allow periodicity (Goldbeter, 1995). In Chapter III: KaiC Phosphorylation Cycle, I examine how non-TTO KaiC oscillations can result from the experimentally observed interactions among the Kai proteins and I predicte the structure of KaiC state transition. I also determine what kind of feedback process controls oscillations in a general closed system. This study has been published as "Predicting regulation of the phosphorylation cycle of KaiC clock protein using mathematical analysis," in the *Journal of Biological Rhythms*.

Chapter II:
Transcriptional Autoregulation by KaiC

Introduction

Circadian rhythms maintain cyclic behavior even under constant conditions without environmental cues. This is called free-run, and is primary evidence that circadian rhythmicity is intrinsic and includes self-sustained oscillators. In model organisms such as *Drosophila*, *Neurospora*, and mouse, circadian rhythms have been shown to be based on cyclic oscillation at a transcriptional level of the clock genes (reviewed in Dunlap, 1999; Young and Kay, 2001). Clock genes form networks of transcriptional interactions including feedback loops to generate autonomous oscillatory dynamics. This TTO model was applied for understanding the cyanobacterial clock mechanism before the discovery of the non-TTO KaiC phosphorylation cycle. In this chapter a study based on this old view that transcriptional autoregulation by KaiC is responsible for cyanobacterial circadian oscillation is demonstrated.

In the cyanobacterium *Synechococcus elongatus PCC 7942*, clock genes *kaiA*, *kaiB*, and *kaiC* have been characterized as indispensable clock regulators (Ishiura *et al.*, 1998). The *kai* genes form a gene cluster, where *kaiB* and *kaiC* are co-transcribed as *kaiBC* mRNA. KaiC plays a central role and exhibits rhythms in transcription, translation, and phosphorylation statuses under continuous light conditions (Iwasaki *et al.*, 2002; Nishiwaki *et al.*, 2000). The other clock proteins KaiA and KaiB modulate KaiC autophosphorylation: KaiA enhances autophosphorylation of KaiC, and KaiB inhibits this action of KaiA (Iwasaki *et al.*, 2002; Kitayama *et al.*, 2003; Williams *et al.*, 2002; Xu *et al.*, 2003).

From the fact that KaiC overexpression consistently reduces the *kaiBC* promoter activity, it has been considered that KaiC negatively regulates *kaiBC*

transcription (Ishiura *et al.*, 1998). Contrarily, KaiA positively regulates transcription as KaiA overexpression induces *kaiBC* transcription in a wildtype strain. KaiA overexpression in the *kaiC*$^-$ strain did not show transcriptional up-regulation, suggesting that KaiC, coupled with KaiA, is involved in the positive limb of transcriptional regulation (Iwasaki *et al.*, 2002). Moreover, KaiC overexpression in a *kaiA*-inactivated (*kaiA*$^-$) strain did not repress and instead gradually induced *kaiBC* expression. KaiA and KaiC appear to regulate *kaiBC* transcription in a cooperative, but unknown way. Considering the fact that KaiA enhances KaiC phosphorylation, it is suggested that this cooperative regulation is realized by KaiC phosphorylation. Indeed, it was observed that overexpression of the nonphosphorylatable KaiC mutant only transiently represses *kaiBC* transcription (Nishiwaki *et al.*, 2004). This result provides proof of the existence of the phosphorylation-dependent switch by KaiC.

In this study, I investigated and predicted the possible mechanisms of transcriptional regulation by KaiC in its phosphorylated state to realize circadian oscillation using a mathematical model. Considering the experimental results, phosphorylated and non-phosphorylated KaiC may have different roles in transcriptional regulation. I developed a mathematical model that included concentrations of phosphorylated and non-phosphorylated KaiC, and *kaiBC* mRNA. I used transcriptional regulation functions that switch their values depending on the amounts of phosphorylated and non-phosphorylated KaiC. I examined all regulation patterns and determined the condition for oscillation by linear stability analysis. First, I determined that there are only two possible patterns in transcriptional regulation that realize circadian oscillation. Second, I verified if the determined conditions could explain the cyanobacterial circadian mechanism, comparing the behavior in computer simulation with the experimentally observed phenotypes. It was suggested that transcriptional

oscillation driven by positive feedback of phosphorylated KaiC is suitable for coupling with the KaiC phosphorylation cycle.

Models

I developed a model that describes interactions in continuous time and states between the clock gene products; *kaiBC* mRNA, KaiA, KaiB, and KaiC. The *kaiBC* level and KaiC phosphorylation are known to exhibit oscillation in a circadian fashion; thus I used a three-variable model as follows,

$$\begin{aligned} \frac{dU}{dt} &= F(N,P) - q_u U \\ \frac{dN}{dt} &= pU - Phos(N,P) - q_n N \\ \frac{dP}{dt} &= Phos(N,P) - q_p P \end{aligned} \quad , \qquad \text{(II-1)}$$

, where U, N, and P are the concentrations of *kaiBC* mRNA, of non-phosphorylated KaiC (NP-KaiC), and of phosphorylated KaiC (P-KaiC), respectively. Since it has been observed that the amount of KaiA in the cytosol of a single cell remains constant at a low level, and that the amount of KaiB is always proportional to that of KaiC (Kitayama *et al.*, 2003), the three-variable model is suitable to consider the oscillatory behavior of the three clock genes.

In the framework used here, I assumed that *kaiBC* transcription is regulated by NP-KaiC and P-KaiC. The transcription rate of *kaiBC* is $F(N,P)$, a function depending on the levels of NP-KaiC and P-KaiC (described later in the subsection). NP-KaiC concentration increases with translation from *kaiBC*. The rate is assumed to be proportional to the level of *kaiBC*, and the rate constant is p. Phosphorylation of NP-KaiC increases P-KaiC, and dephosphorylation of P-KaiC increases NP-KaiC. The total change by these reactions is denoted by $Phos(N,P)$, the phosphorylation/dephosphorylation function depending on the concentrations

of substrates NP-KaiC and P-KaiC (described later in the subsection). The concentrations of KaiA and KaiB are assumed to enhance and attenuate phosphorylation, respectively, and are also included in *Phos*(*N,P*). The degradation rates of *kaiBC*, NP-KaiC, and P-KaiC are assumed to be proportional to their concentrations, with their rate constants being q_u, q_n, and q_p, respectively.

F(*N,P*), The Transcription Function

I assumed that the switching behavior of the transcription function *F*(*N,P*) takes a high or low value in a NP-KaiC- and P-KaiC-dependent manner.

The function *F*(*N,P*) is based on the transcriptional regulation model developed by Mochizuki, a continuous form of a Boolean network (Mochizuki, 2005). For easier understanding, I show the one-dimensional form of the transcriptional regulation function as following,

$$F = \frac{1}{1+\exp\left[\lambda(v-T)\right]} \qquad \text{(II-2)}$$

, where v is the concentration of the regulatory protein and T is the threshold for v. When λ is positive, F takes a value about 0 at the condition $v>T$, and one of about 1 at $v<T$. As v approaches T, F switches from 0 to 1 (or 1 to 0). When λ is negative, the switching pattern is an inverse of the above. λ also determines the steepness of the transition by its absolute value. Here, I improved the function Eq. (II-2) as follows,

$$F(N,P) = \frac{1}{1+\exp\left[\lambda(N\cos\theta + Psin\theta - T)\right]} \qquad \text{(II-3)}$$

Now $F(N,P)$ switches when the sign of $N\cos\theta + Psin\theta - T$ changes. Fig. II-2a shows the two-dimensional space of NP-KaiC and P-KaiC, which is divided in two areas by the straight line of $N\cos\theta + Psin\theta - T = 0$. Similarly to F in Eq. (II-2), $F(N,P)$ continuously takes different values from 0 to 1 depending on the distance of (N,P) from the line as shown in Fig. II-2b, where $(\cos\theta, sin\theta)$ is a normal vector of the threshold line and T is the distance of the line from the origin. By choosing the value $(\cos\theta, sin\theta)$, the relative influences of NP-KaiC and P-KaiC on transcription can be changed.

***Phos*(*N,P*), The Phosphorylation/Dephosphorylation Function**

KaiA is known to enhance KaiC autophosphorylation activity, which is very low without KaiA *in vitro* (Williams *et al.*, 2002). I assumed that KaiC phosphorylation is regulated positively by the concentration of KaiA, and that KaiC's autophosphorylation rate without KaiA is very small and can be ignored. Using these assumptions, the Michaelis-Menten function can be used for KaiC phosphorylation. It was observed that KaiC alone exhibited autophosphatase activity *in vitro*; thus, I assumed that P-KaiC is dephosphorylated in proportion to just its concentration.

Although KaiB is known to attenuate KaiC autophosphorylation, the precise mechanism has not been examined. To investigate all possible mechanisms of chemical reactions between Kai proteins, four types of the function *Phos* that specify the different activities of KaiB were used: (a) KaiB inhibits phosphorylation in a competitive manner, (b) KaiB inhibits phosphorylation in a non-competitive manner, (c) KaiB enhances dephosphorylation, (d) KaiB enhances dephosphorylation, but requires KaiA to do so. KaiB is reported to change the equilibrium state of KaiC phosphorylation only when KaiA is present, *in vitro* as well as *in vivo* (Kitayama *et al.*, 2003; Williams *et al.*, 2002; Xu *et al.*, 2003). In

this regard, (a) and (b) seem more plausible than (c). Type (d) is an improved function of (c). All types contain KaiA-enhanced phosphorylation and spontaneous dephosphorylation of KaiC. The details and the formulae are shown in Appendix II-A.

Results

Analysis

I investigated the conditions of gene regulation to generate oscillation using linear stability analysis of the model. The equilibria of the model and the condition of the destabilization by Hopf bifurcation were determined numerically (Appendix II-B) changing parameters in the transcription function, the phosphorylation/dephosphorylation function and other parameters in Eq. (II-1). I confirmed that the dynamic trajectory of this model shows oscillation for all the parameter sets satisfying the conditions for Hopf bifurcation.

Fig. II-3 shows the conditions for generating oscillation on the two-dimensional parameter space, where the horizontal axis is the angle of the threshold line of transcriptional switching, and the vertical axis is the phosphorylation rate. I used type (b) *Phos* in this analysis. The figure shows that the instability causing the cyclic behavior is observed only in very restricted conditions on the two-dimensional space. There are two regions separated along the horizontal axis of the transcriptional pattern, suggesting that there are two distinct mechanisms.

In one region, P-KaiC induces transcription, and in the other, P-KaiC represses transcription. Transcriptions in both the regions slightly depend on the NP-KaiC concentration. Fig. II-4 illustrates the functional schemes of the two distinct regulation patterns derived from the conditions of the parameter sets in the two regions. I call the former picture the Transcriptional Activation Model (TAM) and the latter the Transcriptional Repression Model (TRM). TRM is easy to understand. It follows the principles of self-repression typically used for understanding the circadian clocks of various species (Hardin *et al.*, 1990).

On the other hand, TAM does not include self-repression of transcription and is regulated positively by KaiC. This model may be contrary to intuition. However, the dynamics following this model can generate stable periodic oscillation in computer simulations, and show some rather favorable properties to explain the experimentally observed phenomena than the counterpart model. In fact, it may be possible to understand this model by focusing on the dephosphorylation enhanced by KaiB, which is co-expressed with KaiC, and may act as the regulator of indirect negative feedback. To realize this picture of "indirect negative feedback", the phosphorylation and dephosphorylation process should be far from equilibrium, and may show strong oscillations in the dynamics of circadian rhythms.

Fig. II-5 shows dynamic changes in the net phosphorylation rate *Phos*, which includes both the phosphorylation and, its inverse, the dephosphorylation processes. In TAM, the amplitude of *Phos* is large and the value changes from positive to negative in dynamic oscillation. The large dephosphorylation rate in TAM enables *Phos* to take a negative value depending on the KaiB level. A positive *Phos* means that the phosphorylation rate is larger than the inverse process, while a negative *Phos* means the opposite situation. The alternation of phosphorylation-dominant and dephosphorylation-dominant phases is observed only in TAM. The period of this alternation synchronizes with oscillation of the whole dynamic system. In TRM, *Phos* takes only a positive value and its amplitude is small. This suggested that big changes in *Phos* are not necessary in TRM.

Fig. II-3 also shows the difference in phosphorylation rates between the models. The phosphorylation rate in TAM distributes higher values on average than TRM. The same property in the phosphorylation rate was observed even

when I used different types of phosphorylation functions. The exceptions were the case when I used type (a) or (d) (Table II-1), where I did not observe oscillation of TAM.

Fig. II-6 shows examples of the dynamic trajectory of NP-KaiC and P-KaiC and the nullclines of dP/dt and $F(N,P)$ in the space of NP-KaiC and P-KaiC in typical TAM (Fig. II-6a) and TRM (Fig. II-6b). In TRM, anticlockwise-oscillation appears around the region where the nullcline of dP/dt increases with NP-KaiC. In TAM, on the other hand, clockwise-oscillation appears around the region where the effect of substrate density on phosphorylation is saturated and the nullcline of dP/dt decreases with NP-KaiC from the dephosphorylation effect of KaiB (proportional to $N+P$). The difference in the shape of the *Phos* nullcline corresponds to the difference in the rate of phosphorylation. The phosphorylation rate in TRM needs to be low to generate oscillation. The phosphorylation rate in TAM needs to be high.

Computer Simulation

I numerically analyzed the models by computer simulation to confirm the results of linear stability analysis. The simple explicit difference method was used for calculations of differential equations Eq. (II-1). Fig. II-7 shows typical dynamic changes of the gene products, where the same parameter values were used as in Fig. II-5. The horizontal axis is time and the vertical axis is the concentrations of *kaiBC*, NP-KaiC and P-KaiC. The dynamic changes obtained from type (c) *Phos* exhibited oscillation around the equilibrium shown in Fig. II-5. The *kaiBC* level, total amount, and the phosphorylation level of KaiC repeatedly rise and fall with periodicity (Fig. II-7), as in cyanobacteria. All the dynamics showed periodic oscillations in the computer simulation when the parameter values

satisfied the condition of instability determined in the previous section. The only exceptional weak result was the case when type (b) *Phos* was used. In this case, dynamic changes calculated by simulation showed very low amplitude of the P-KaiC oscillation under conditions where oscillation was expected from the concept of TAM. In TRM, similar oscillation patterns were obtained using any type of *Phos*.

In TAM, the transcription phase is in phase with that of phosphorylation, contrary to the experimental result (Fig. II-7a). On the other hand, TRM generates realistic oscillations in terms of the transcription phase pattern, phosphorylation and the total amount of KaiC protein (Fig. II-7b).

It is known that KaiC phosphorylation is very slow process. *In vitro* autokinase assay revealed that KaiC is autophosphorylated from 40 % to 80 % after 6 hours of incubation with KaiA (Tomita *et al.*, 2005). This low phosphorylation rate is a characteristic property of a *kai* oscillator. In the computer simulation, the phosphorylation rate was shown to be low in both models, at least in all the parameter sets I used. To keep the oscillation period to 24 h, both models can generate oscillations with very low phosphorylation rates (data not shown).

Experimental studies such as overexpression and deletion of *kai* genes have been carried out to investigate their effects on the transcriptional regulation of *kaiBC* (Ishiura *et al.*, 1998; Iwasaki *et al.*, 2002). Many period mutants showing longer or shorter periods have been observed and their mutated locus and functional differences identified (Xu *et al.*, 2003). I could simulate the metabolic changes of these mutations by controlling variables or parameter values in a computer simulation. I compared behavior in TAM and TRM with these observed phenotypes, and tested which model could better explain the behaviors of mutants (Table II-2). For each model, I used sets of parameter values for which

the model generated typical periodic oscillations.

~KaiC disruption and overexpression~

It is reported that KaiC overexpression repressed *kaiBC* expression to a trough level of oscillation in an intact cell (Ishiura *et al.*, 1998). The effect of KaiC overexpression was simulated by substituting $U+u$ for U in *dN/dt*. The differential equation then becomes;

$$\frac{dN}{dt} = p(U+u) - Phos(N,P) - q_n N \qquad \text{(II-4)}$$

, where u is an increase of *kaiC* by overexpression. I determined the u value so that it increased KaiC (N+P) to 10 ~ 100 times larger than the original in the computer simulation. By overexpression, NP-KaiC greatly increased though P-KaiC increased only a little. This was because the phosphorylation rate that is increasing with KaiC saturates and reaches a finite value, and KaiC's turnover increases rather linearly with KaiC without saturation. In TAM, the result depended on a small difference in transcription pattern. When NP-KaiC induced transcription, the *kaiBC* level abolished oscillation and took a minimal value from *kaiC* overexpression. In this case, the transcriptional threshold at the high NP-KaiC value was very high for P-KaiC, and transcriptional repression lasted continuously. When NP-KaiC did not affect on transcription in TAM, the *kaiBC* level is kept oscillating in a large amplitude by *kaiC* overexpression. In TRM, the *kaiBC* level took a minimal value from *kaiC* overexpression, regardless of the switching pattern of transcription.

Next, I examined the *kaiC*$^-$ mutant, which can be simulated by fixing N and P to zero in a computer simulation. It is reported that the *kaiC*$^-$ mutant reduces *kaiBC*

expression to ~20 % of the wildtype strain (Iwasaki *et al*., 2002). The *kaiBC* level abolished oscillation and took small and maximal values in TAM and Transcriptional Repression Model, respectively. These results suggested that TAM successfully explains the function of KaiC.

~KaiA inactivation and overexpression~

The *kaiA*$^-$ mutant can be simulated by fixing the KaiA activity rate to zero in numerical calculation. The result of TAM and TRM showed the minimal and the maximal level of *kaiBC* expression, respectively. KaiA overexpression was simulated by increasing the KaiA activity rate k_a during the dynamic change. Both models showed the maximal and minimal *kaiBC* levels, respectively. These results indicated that KaiA-mediated induction of *kaiBC* can be explained by TAM, but cannot be explained by TRM. Experimental studies have shown that KaiA-mediated activation of *kaiBC* is KaiC dependent (Iwasaki *et al.*, 2002). In TAM, KaiA overexpression in the *kaiC*$^-$ mutant did not induce *kaiBC* expression differently from KaiA overexpression in wildtype, showing that this model explained the KaiA effect depending on KaiC.

KaiA-KaiC cooperation has also been investigated by examining KaiC overexpression in the *kaiA*$^-$ mutant (Iwasaki *et al.*, 2002). The phenotype of *kaiA*$^-$ showed severely repressed *kaiBC* expression, and KaiC overexpression in this mutant cells showed slow and slight increase of *kaiBC* expression. This result is consistent with the fact that overexpression of the non-phosphorylatable KaiC mutant transiently represses and gradually increases transcription (Nishiwaki *et al*., 2004). In the computer simulation of TAM, both wildtype overexpression of the *kaiA*$^-$ strain and KaiC mutant overexpression resulted in a minimal level of transcription, indicating that this model does not perfectly explain cooperative KaiA-KaiC functions. TRM failed to explain transcriptional repression by the

kaiA$^-$ mutant.

~KaiB disruption~

The *kaiB*-disrupted (*kaiB*$^-$) mutant was simulated by fixing the KaiB activity rate (k_b in type (c) *Phos* and k_n in type (b) *Phos*) to zero. In TRM using type (b) or (c) *Phos*, KaiB disruption did not cease the oscillations. Using type (a) or (d), the dynamics of *kaiBC* converged to a static state at an intermediate value when the KaiB activity rate was fixed to zero. These results were inconsistent with the observed phenotype. In TAM, on the other hand, *kaiBC* oscillation stopped and converged to a static state at the maximum value in the computer simulation of the *kaiB*$^-$ mutant. This seemed e consistent with the actual phenotype of *kaiB*$^-$, which exhibited a slow increase of *kaiBC* level. The persistence of oscillation under the *kaiB*-disrupted condition observed in TRM suggested that KaiB is not essential in this model.

~Period mutants~

I investigated the effect of increases or decreases in parameter values on the oscillating period (Fig. II-8). It is reported that the *kaiA2* mutation in *kaiA* (the A30a strain) shows a 70 % reduction of KaiC phosphorylation (Iwasaki *et al.*, 2002), and causes a longer period, to ~30 h (Ishiura *et al.*, 1998). The *kaiB2* mutation in KaiB (the B22a strain) exhibits short period phenotype (Ishiura *et al.*, 1998), by decreasing the negative effect on KaiC phosphorylation (Xu *et al.*, 2003). It is reported that in the C22a (*kaiC1* mutation) and C55a strains, NP-KaiC is degraded quickly and slowly, and exhibits 22 h and 55 h period phenotypes, respectively (Ishiura *et al.*, 1998). Half-lives of non-phosphorylated KaiC are 8.8 h, 6.7 h and 13.9 h in wildtype, C22a and C55a, respectively; though P-KaiC stability was at a the similar level in all strains (Xu *et al.*, 2003).

In TRM using type (a) *Phos*, all these period mutant phenotypes were realized by computer simulation. Fig. II-8b shows the effect of the KaiA activity rate k_a that shortens the period as it increases. Decreasing k_a from 100 to 70, the period became 1.36 times longer. This result seemed consistent with the A30a phenotype, exhibiting a period 1.25 times longer than the wildtype strain. In this model, a decrease in the KaiA activity rate seemed to lead to a delay in the negative effect from P-KaiC, resulting in a longer period. Fig. II-8d shows the effect of the KaiB activity rate k_c that lengthens the period as it increases. This result was consistent with the experimentally observed phenotype of the B22a strain. A similar result was obtained using type (d) *Phos*, but not when using types (b) or (c), which do not have dynamic regulation by KaiB. Thus changing the KaiB activity rate had no effect on the period (data not shown). Fig. II-8f shows the effect of the NP-KaiC degradation rate q_n that shortens the period as it increases. The degradation rate of NP-KaiC in the C22a and C55a strains can be calculated from the half-lives of NP-KaiC in these strains; rates were 131 % and 63 %, respectively, of wildtype KaiC. I examined the period in TRM using q_n=0.131 and 0.063, and obtained a period 0.95 and 1.07 times, respectively, longer than in the model using q_n=0.1. In TRM, the effect of q_n on the period can be explained qualitatively, but not quantitatively.

In TAM, the effect of the activity rates of KaiA and KaiB, and that of the KaiC degradation rate cannot be realized with a wide range of parameter values; though they may be realized in limited parameter conditions. Fig. II-8a shows the effect of k_a that lengthens the period as it increases. The period may become shorter as the KaiA activity rate increases, but only in limited conditions (Fig. II-8a). Fig. II-8c shows the effect of the KaiB activity rate k_b. When NP-KaiC did not affect on transcription, k_b shortened the period as it increases. When the ratio of P-KaiC and NP-KaiC regulates transcription, decreasing the KaiB effect

shortens the period, thus explaining the effect of the KaiB mutation on the period. Fig. II-8e shows the effect of the NP-KaiC degradation rate q_n that shortens the period as it increases. I examined the period in TAM using q_n=0.262 and 0.126, and obtained periods 0.91 and 1.21, respectively, times as long as the model using q_n=0.2 (Fig. II-8e). The effect of q_n on the period can be explained better in TAM than in TRM.

~Disruption by cell division or cell elongation~

It has been reported that rapid cell division and chromosome duplication occur within one circadian period in cyanobacteria, breaking the paradigm of biological clocks (Kondo *et al*., 1997). I investigated if sustained oscillations in my models could continue when the amounts of KaiA, KaiB, and KaiC were reduced during oscillation in a computer simulation. It was observed in TAM that oscillations persisted after the reduction of Kai proteins (Fig. II-9a), shifting the orbit of the cycle within the variable space of the dynamics (Fig. II-9c). When the same parameter set as used in Fig. II-5 was used, even 90 % reduction did not interrupt oscillations in TAM. Moreover, a 50 % reduction barely affected on the oscillating period, resulting in >92 % of the original period, suggesting that TAM was robust against fluctuations of protein concentrations (Fig. II-9b). On the other hand, oscillation in TRM was attenuated by a reduction of Kai >25 %, indicating that this model was less robust than the other model (Fig. II-9d). Furthermore, the oscillation period was vulnerable in this model, which was extended to 113 % by 20 % reduction (Fig. II-9b). Similar results were observed for each model with the other parameter sets I tested (data not shown).

These results can be explained considering the intersection of the line of the transcriptional threshold and that of the nullcline of *dP/dt* (Fig. II-9c and 9d). The transcriptional threshold is not affected by the change in the concentrations of Kai

proteins. The nullcline of *dP/dt* changed its shape mainly along the vertical axis with changes in the concentration of KaiA. In TAM, where the transcriptional threshold increased with NP-KaiC concentration, the change in the shape of the *dP/dt* nullcline altered the position of the intersection. However, the angle of the lines governing the dynamics at the intersection did not change even with a wide range of protein concentrations. In TRM, however, where the transcriptional threshold was parallel to the NP-KaiC concentration, the angle of the nullclines at the intersections changed with changes in protein concentrations. When the reduction of Kai proteins was large enough, the transcriptional threshold and the nullcline of *dP/dt* did not intersect in this model.

The robustness of TAM against Kai concentrations suggested that this model was more likely to express the actual mechanism of the cyanobacterial circadian clock than TRM.

In conclusion, it was revealed that TAM reproduced most phenotypes in cyanobacteria, suggesting that for the most part KaiA, KaiB, and KaiC work properly. However, TRM reproduced only half of the phenotypes observed in the experimental studies.

Discussion

In this study, I developed a dynamic model of the *kai* TTO mechanism and numerically examined its behavior. It was demonstrated that there were only two possible transcriptional regulations generating oscillations of the *kai* genes: TAM and TRM. The former provides a picture of the network generating circadian oscillations, where transcription is induced positively by the gene products and does not include direct negative feedback regulation.

The mathematical framework in this chapter never explained the non-TTO KaiC phosphorylation cycle, which corresponds to the situation where the transcription and degradation rates ($F(N,P)$, q_n, and q_p) equal zero (data not shown). Meanwhile, under natural conditions, cyanobacteria utilized Kai oscillators both in daylight and after dark, suggesting that the TTO and non-TTO cycles coexist in cyanobacteria. Thus, transcriptional regulation should be compatible to the KaiC phosphorylation cycle in terms of phosphorylation dynamics. Fig. II-5a shows that *Phos* oscillates in a large amplitude and takes positive and negative values in turn in TAM. The negative value of *Phos* indicates the dephosphorylation phase. The P-KaiC/NP-KaiC ratio also oscillates in a large amplitude in this model (Fig. II-7a). Accordingly, TAM is more likely to be involved in non-TTO KaiC phosphorylation. In TRM, *Phos* always takes a positive value (Fig. II-5b) and P-KaiC stays at about the same level (Fig. II-7b).

The inhibitor-activator oscillatory model gives us the simplest concept of oscillatory structures. In TAM, P-KaiC and KaiB can be recognized as activator and inhibitor, respectively. P-KaiC induced *kaiBC* transcription and consequently

increased KaiB and itself. KaiB attenuated KaiC phosphorylation, resulting in transcriptional repression. TRM can also be compared to the inhibitor-activator model by inversely interpreting the players.

The presence and the function of positive feedback in circadian rhythms have been discussed in experimental studies and mathematical models (Allada, 2003; Preitner *et al.*, 2002). In *Drosophila*, *Pdp-1* is activated by CLK, and PDP-1 in turn activates *Clk*. This positive feedback loop is suggested to allow for multiple inputs and outputs at different phases (Allada, 2003). In a mammalian circadian oscillator, the heterodimer BMAL1/CLOCK activates transcription of the *Per*, *Cry*, and *Rev-erbα* genes. PER and CRY form a complex with CKIε/δ and inhibit REB-ERBα synthesis repressing *Bmal1* transcription. This process contributes to the robustness of the clock (Preitner *et al.*, 2002). In both cases, positive feedback regulation works in combination with some other mechanisms including negative feedbacks, suggesting that positive feedback may act as the supporting mechanism to stabilize periodic behavior. On the other hand, TAM did not include direct negative regulations. This result proved that positive feedback itself can be the responsible mechanism for generating periodic oscillation.

Though type (d) *Phos* function is an improved version of type (c), there is a large difference in terms of the dephosphorylation dynamics. In type (d), both phosphorylation and dephosphorylation processes require KaiA. As NP-KaiC accumulated, the dephosphorylation rate decreased because NP-KaiC enhanced phosphorylation and depleted KaiA. The oscillation in TAM required a high dephosphorylation rate when NP-KaiC concentration was high, and thus was impossible by type (d), but possible by type (c).

In *Neurospora* and *Drosophila*, the stability of the clock proteins, Period and

Frequency, is modulated by their rhythmic phosphorylation to fit circadian rhythms (Young and Kay, 2001). Though the effect of KaiC phosphorylation on its stability remains unclear, there are some reports on the correlation between phosphorylation status and KaiC stability (Imai *et al.*, 2004; Xu *et al.*, 2003). Xu *et al*. suggested that the stability of P-KaiC is lower than that of NP-KaiC, using a transient KaiC overinducer in the *kaiC*$^-$ strain. On the other hand, Imai *et al*. reported that KaiC degradation is suppressed during the mid-subjective night, when P-KaiC is highly accumulated. I examined the importance of NP-KaiC and P-KaiC stability separately by determining the q_n and q_p values that can generate oscillation using type (c) *Phos* (data not shown). It was revealed that oscillation in TAM depended on the stability of NP-KaiC, which is not important in TRM. As well, the stability of P-KaiC should be lower in TRM than in TAM. In the latter, where P-KaiC-induced KaiB expression indirectly represses transcription, NP-KaiC and P-KaiC should be stable until they induce KaiB expression to generate oscillation. Meanwhile in TRM, where P-KaiC directly repressed transcription, P-KaiC should be degraded quickly to avoid convergence to the attractor. No tendency was observed in q_n/q_p in both models.

TAM is expected to reflect the actual mechanism generating transcriptional oscillation. At the same time, the limitations of this model were clearly shown. The difference in the phosphorylation level of KaiC was not sufficient to explain circadian oscillation in cyanobacteria; other unknown factors have to be included to explain all the observed behavior of transcriptional regulation.

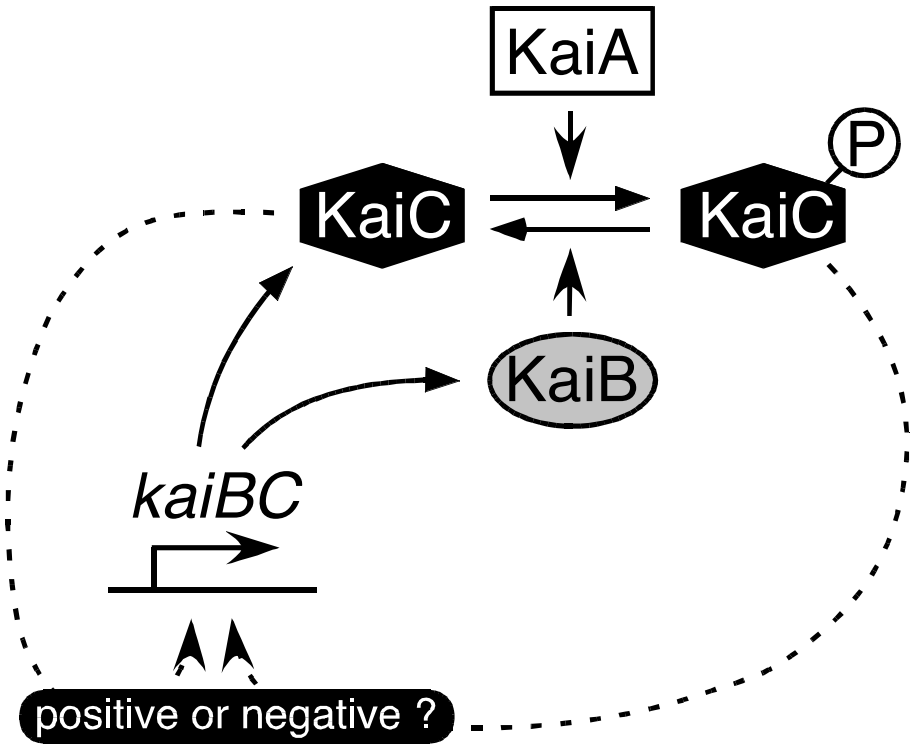

Fig. II-1

Schematic view of transcription/translation-based autoregulatory loop of the *kai* oscillator in cyanobacterial circadian rhythms. KaiC has autokinase and autophosphatase activities. The genes of *kaiB* and *kaiC* form an operon, and *kaiBC* mRNA, KaiB and KaiC protein accumulates in a circadian fashion in free-running conditions. KaiA enhances KaiC phosphorylation, while KaiB antagonizes the actions of KaiA. KaiC phosphorylation also shows circadian oscillation. KaiC had been thought as negative regulator of *kaiBC* transcription. However, it has revealed recently that it may regulate transcription both positively or negatively.

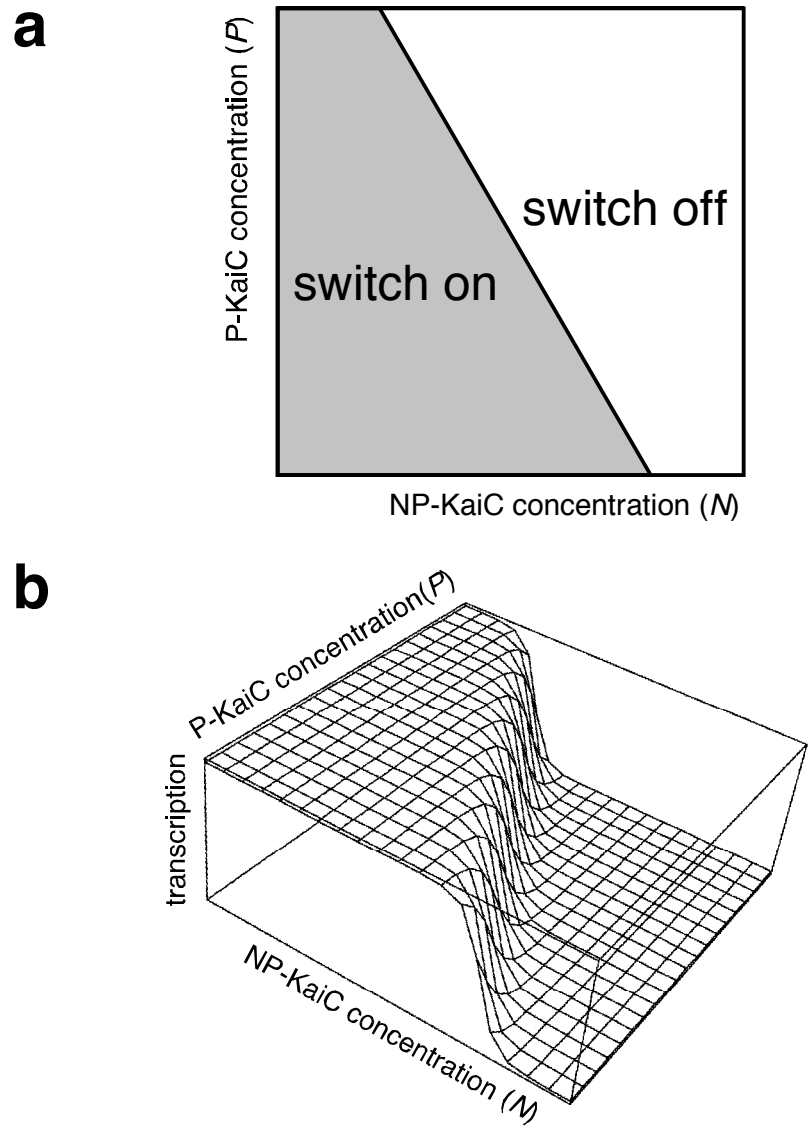

Fig. II-2

Examples of transcriptional functions when transcription is controlled by nonphosphorylated KaiC (NP-KaiC) and phosphorylated KaiC (P-KaiC). Transcription is active (On) when NP-KaiC and P-KaiC are less abundant, and inactive (Off) when both are abundant. (a) Threshold of transcriptional switching, which is determined by a line $N\cos\theta + P\sin\theta - T = 0$, is plotted on the two-dimensional space of the NP-KaiC concentration (N), the P-KaiC concentration (P). (b) The transcriptional level $F(N,P)$ is plotted as a function of the two-dimensional space. $F(N,P)$ switches continuously near the threshold.

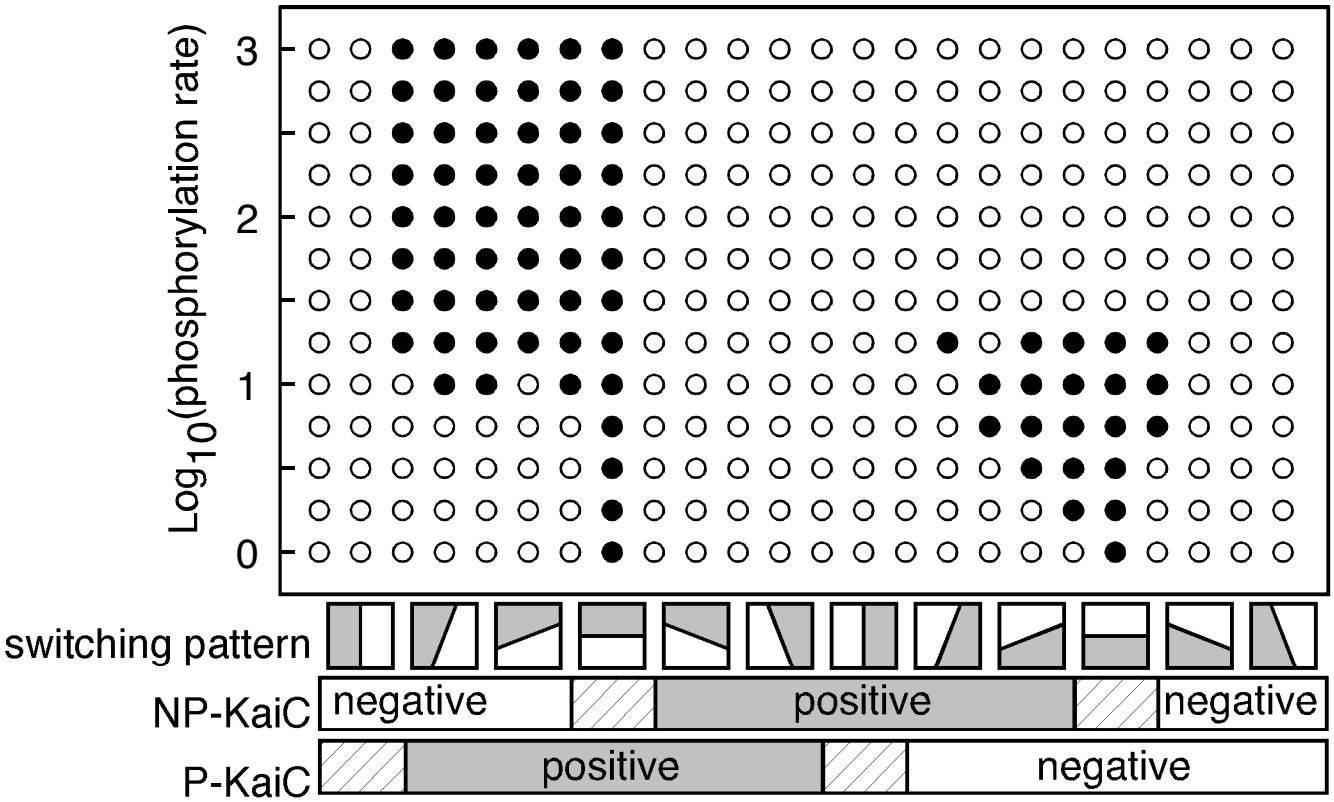

Fig. II-3

The result of linear stability analysis using type (c) *Phos*. The horizontal axis is θ, the angle of the threshold line of transcriptional switching, and the vertical axis is k_a, the phosphorylation rate. The θ specifies patterns of the transcriptional regulation, which are shown schematically below the horizontal axis. Along the horizontal axis, the regulation changes continuously; effects of NP-KaiC and P-KaiC are positive or negative. Open circles indicate conditions of the transcription and phosphorylation rates where oscillation never occurs, and filled circles indicate where oscillation can occur. In this analysis, we assumed that $q_n=q_p$. The result was obtained when $\lambda=5$, $0<\theta<2\pi$, $-15<T<15$, $q_u=1$, $0.05<q_n<.8$, $5<p<80$, $1<k_a<10^3$, $10^{-3}<k_b<1$, $k_m=0.1$, $k_{mb}=0.1$, $k_d=0$.

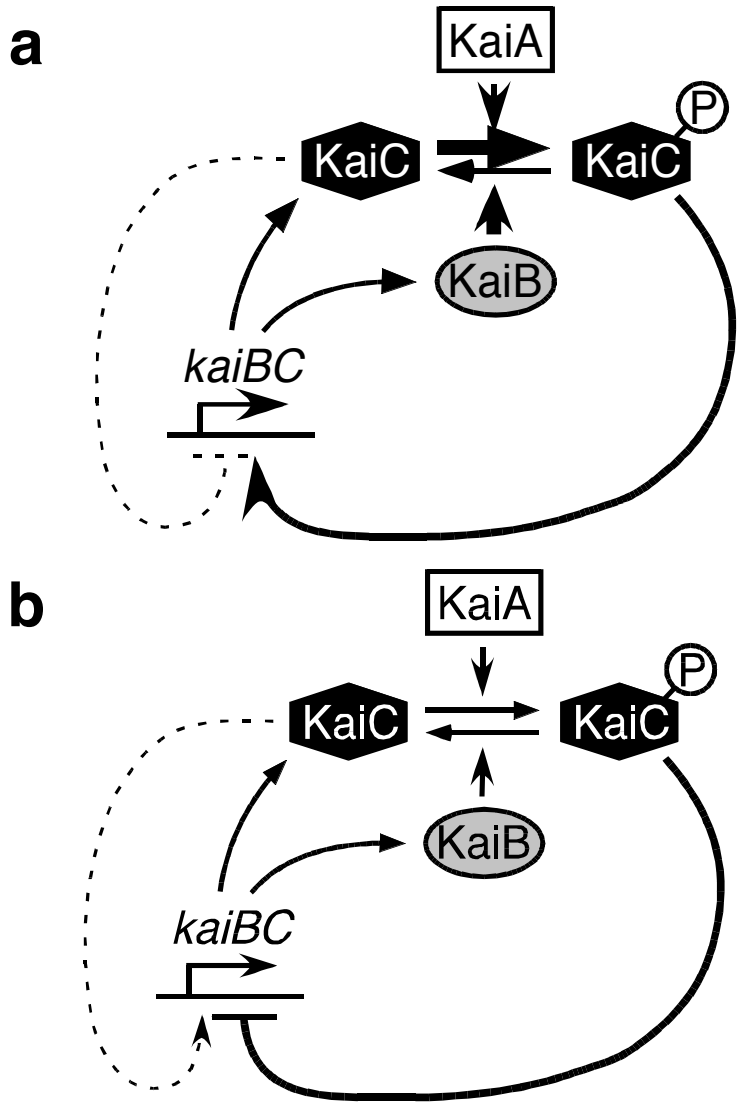

Fig. II-4

Functional schemes of two models corresponding to the parameter regions producing the cyclic behaviors shown in Fig. II-3. (a) The Transcriptional Activation Model, where P-KaiC induces kaiBC transcription. NP-KaiC does not affect on transcription, or has a small effect of repressing transcription. The phosphorylation rate k_a and the non-competitive inhibition rate k_n are high. (b) The Transcriptional Repression Model, where P-KaiC represses *kaiBC* transcription. NP-KaiC induces transcription weakly, or does not affect on transcription. The KaiA activity k_a and the non-competitive inhibition rate k_n are low.

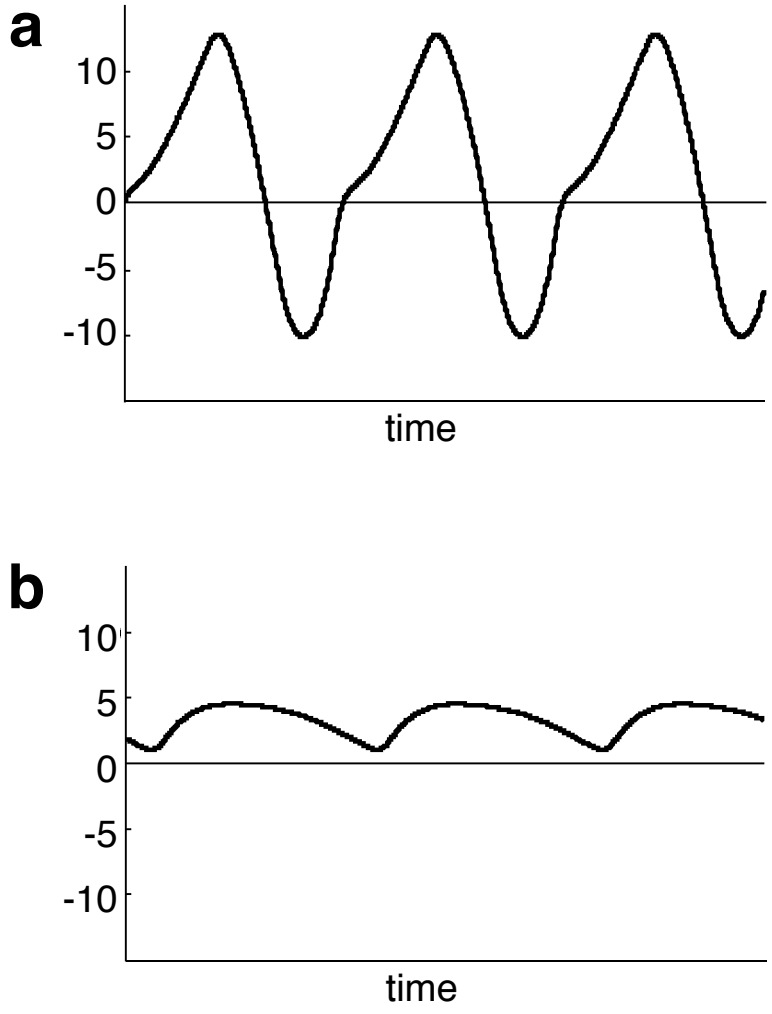

Fig. II-5

Example of temporal changes in *Phos*. The horizontal axis is the time and the vertical axis is the *Phos* value. (a) The Transcriptional Activation Model. The *Phos* changes periodically. The amplitude is large and takes positive and negative values. The result was obtained when q_u=1, p=20, q_n=0.2, q_p=0.2, λ=-5, θ=3/4π, T=1, k_a=50, k_m=0.14, k_b=1.6, k_{mb}=0.14, k_d=0. (b) The Transcriptional Repression Model. The *Phos* shows periodic oscillation, though the amplitude is small and the value is always positive. The result was obtained when q_u=1, p=20, q_n=0.2, q_p=0.2, λ=5, θ=π/2, T=15, k_a=6, k_m=5, k_b=.01, k_{mb}=10, k_d=0.

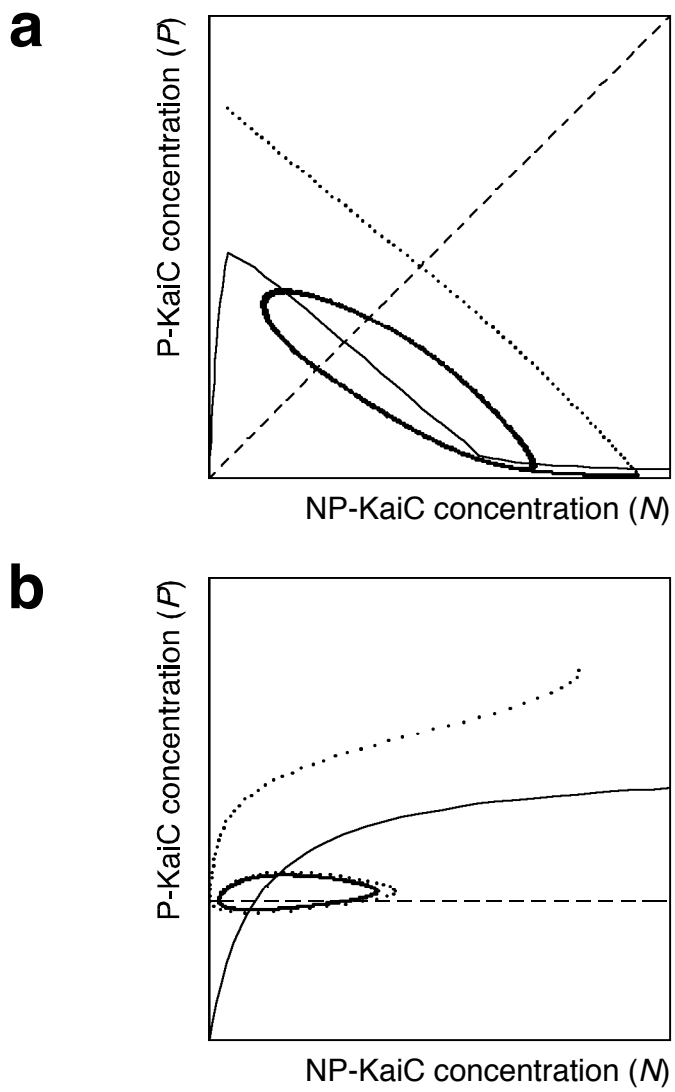

Fig. II-6

Examples of dynamical changes of NP-KaiC and P-KaiC (dotted lines) using type (c) *Phos*. The horizontal axis is the NP-KaiC concentration (*N*) and the vertical axis is the P-KaiC concentration (*P*). Solid curves are the nullclines of *dP/dt*, dashed straight lines are the transcriptional thresholds. The parameter values are shown in Fig. II-5. (a) In the Transcriptional Activation Model, the dynamical trajectory shows clockwise cycle on the NP-KaiC and P-KaiC space. Transcription is active (on) above the threshold and inactive (off) below the threshold. (b) In the Transcriptional Repression Model, the dynamical trajectory shows anticlockwise cycle on the NP-KaiC and P-KaiC space. Transcription is inactive (off) above the threshold and active (on) below the threshold.

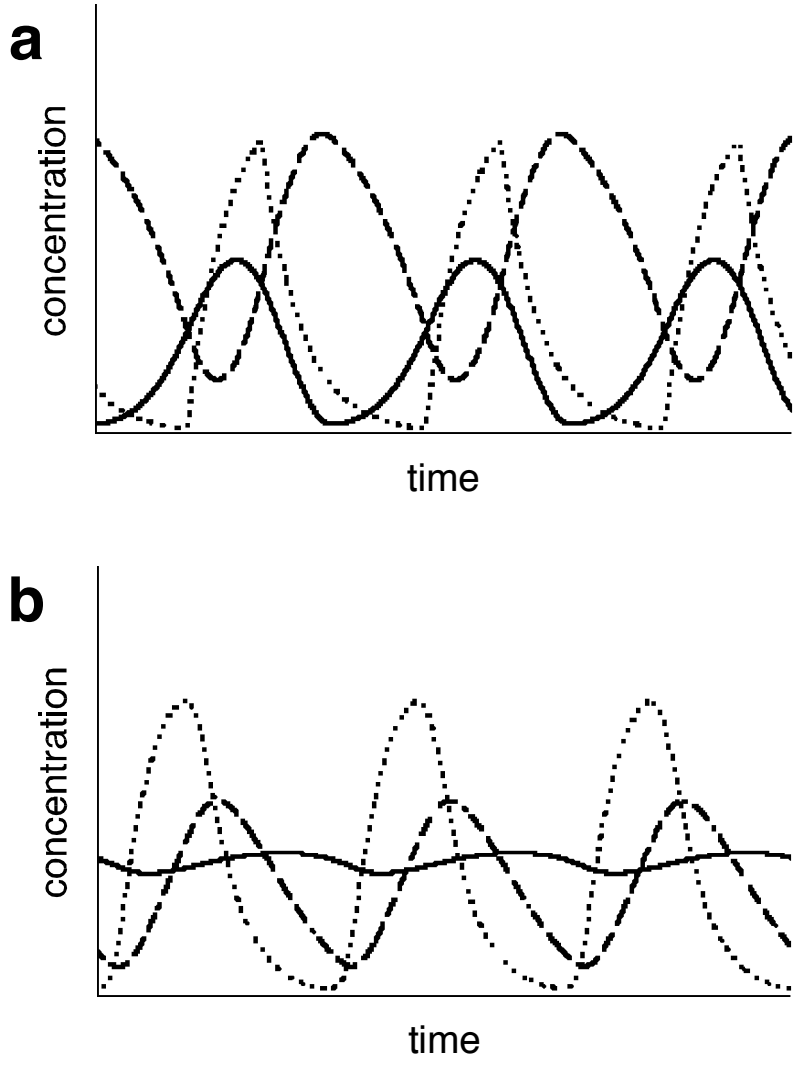

Fig. II-7

Example of temporal changes of *kaiBC,* NP-KaiC and P-KaiC. The horizontal axis is the time and the vertical axis their concentration. Dotted lines, *kaiBC*; dashed lines, NP-KaiC; solid lines, P-KaiC. (a) The Transcriptional Activation Model. (b) The Transcriptional Repression Model. The parameter values are shown in Fig. II-5.

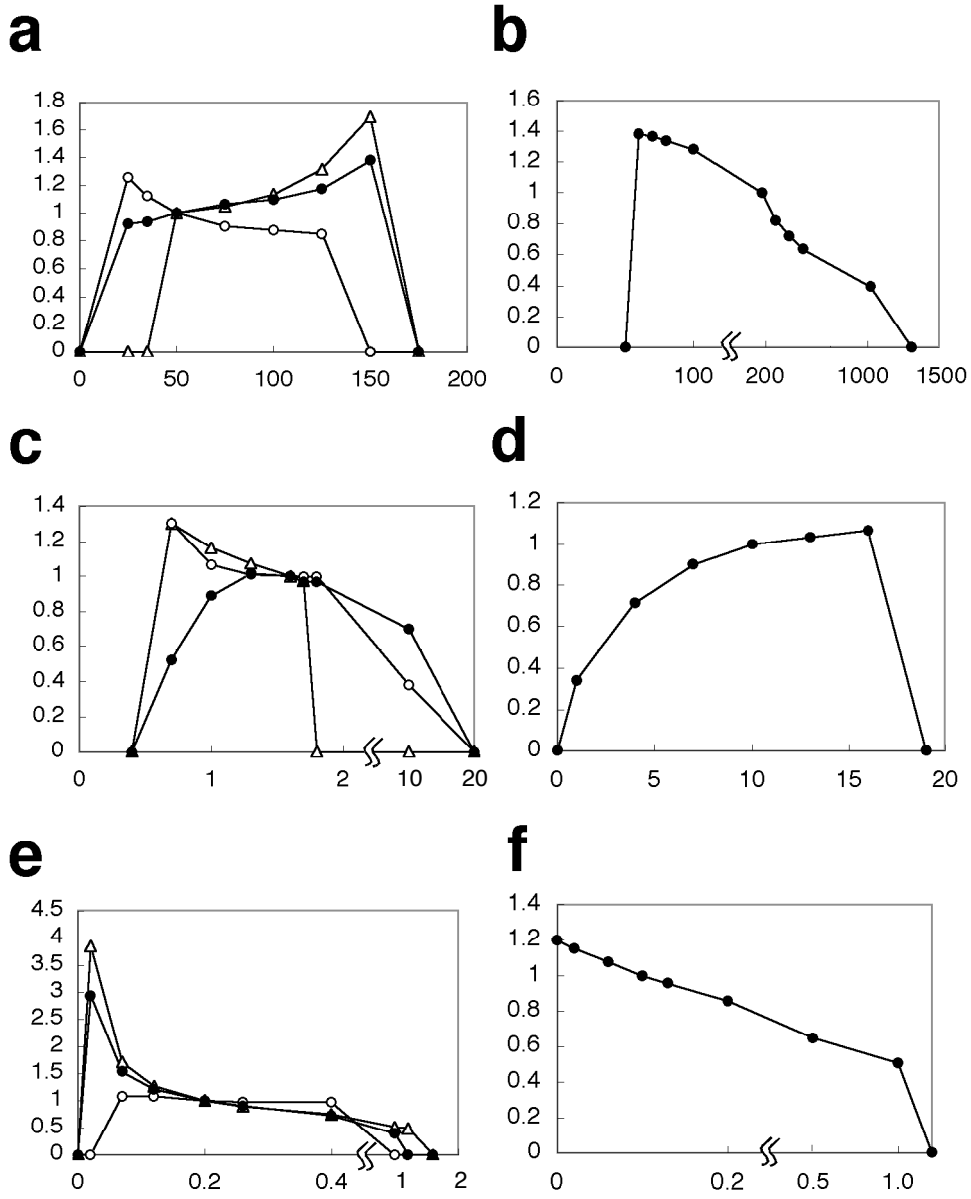

Fig. II-8

Effects of parameter values on period. The vertical axis is the relative length of oscillation period compared to wildtype shown in Fig. II-7. The period 0 means that oscillation does not occur using the parameter value. The horizontal axis is the changes in KaiA activity k_a ((a) and (b)), KaiB activity k_b ((c) and (d)), and the KaiC degradation rate q_n ((e) and (f)). (a), (c), (e) The Transcriptional Activation Model of type (c) *Phos*. Filled circle, parameter values shown in Fig. II-5; open circle, same as filled circle except for $\theta=\pi/2$, $T=2$; open triangle, same as filled circle except for $\lambda=-5$, $\theta=\pi/2$, $T=18$. (b), (d), (f) The Transcriptional Repression Model of type (a) *Phos*. The result was obtained when $q_u=1$, $p=20$, $q_n=0.2$, $q_p=0.1$, $\lambda=5$, $\theta=\pi/2$, $T=18$, $k_a=100$, $k_m=1$, $k_c=10$, $k_d=0.1$.

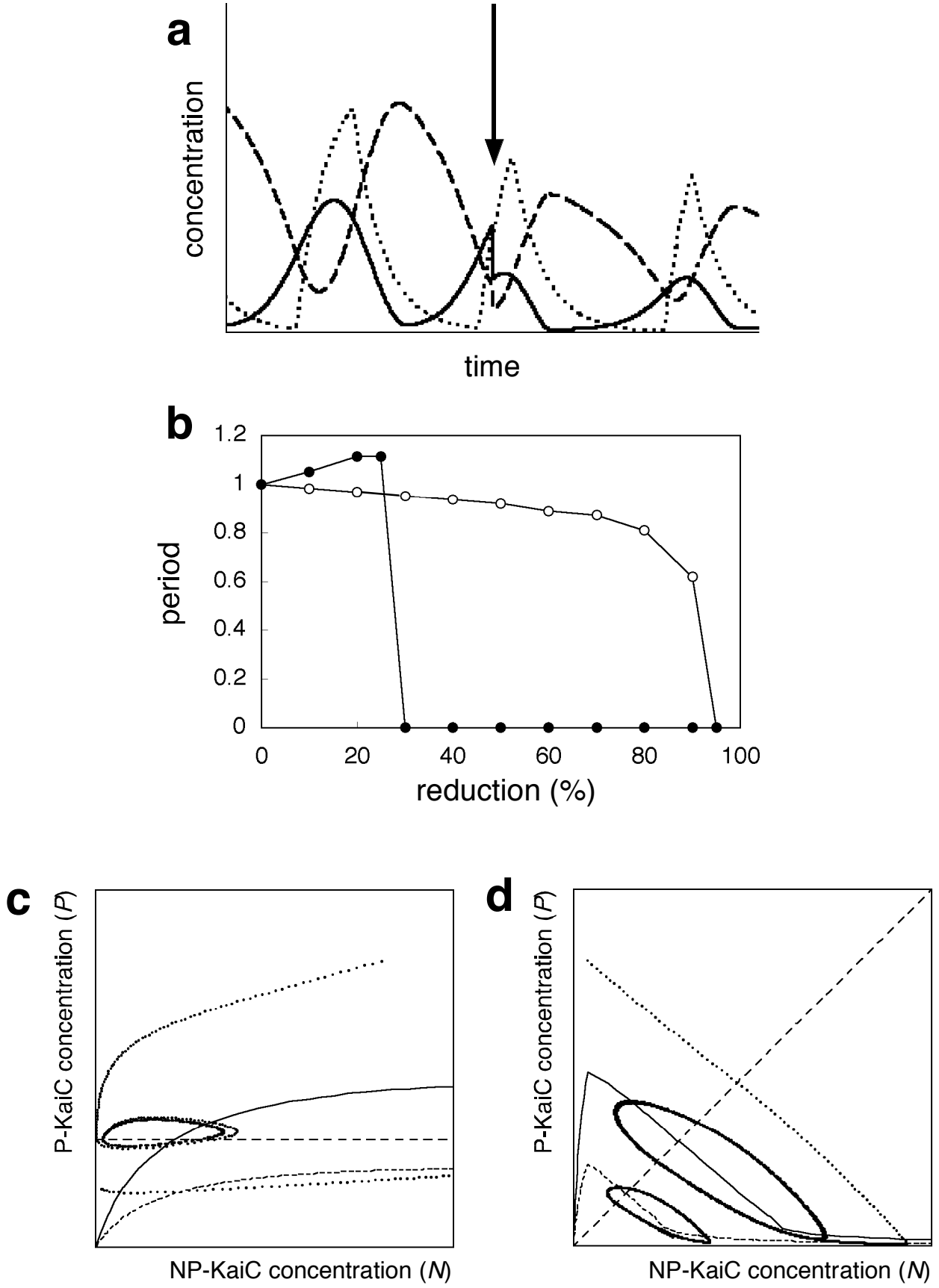
a
concentration
time
b
period
reduction (%)
1.2
1
0.8
0.6
0.4
0.2
0
0
20
40
60
80
100
c
P-KaiC concentration (P)
NP-KaiC concentration (N)
d
P-KaiC concentration (P)
NP-KaiC concentration (N)

Fig. II-9

Computer simulation of the disruption of protein concentration by cell division or cell elongation in the Transcriptional Activation Model. The original parameter values are the same as shown in Fig. II-5. (a) Example of temporal changes of kaiBC, NP-KaiC and P-KaiC in the Transcription Activation Model. The horizontal axis is the time and the vertical axis their concentration. Dotted lines, *kaiBC*; dashed lines, NP-KaiC; solid lines, P-KaiC. The KaiA, KaiB and KaiC concentrations were reduced to 50 % (arrows). (b) Effects of reduction of the Kai protein concentrations on period. The vertical axis is the relative length of oscillation period compared to original condition. The period 0 means that oscillation does not occur using the parameter value. The horizontal axis is the reduction of the protein concentrations. Open circle, the Transcriptional Activation Model; filled circle, the Transcriptional Repression Model. (c, d) Examples of dynamical changes of NP-KaiC and P-KaiC (dotted lines). The horizontal axis is the NP-KaiC concentration (N) and the vertical axis the P-KaiC concentration (P). Dashed straight line is the transcriptional threshold and transcription is active (on) above the threshold and inactive (off) below the threshold. The solid curve is the nullclines of *dP/dt*, and the dashed curve the nullclines of *dP/dt* after 50 % reduction of the concentrations of the Kai proteins. (c) The Transcriptional Activation Model. The dynamical trajectory shifts to the smaller circle after reduction of the protein concentrations. (d) The Transcriptional Repression Model. The nullclines of *dP/dt* no longer intersect the transcriptional threshold after the 50 % reduction and the system converges to a steady state at (N,P)=(88.4, 11.5).

Phos	KaiB's function	TAM	TRM
(a)	competitive inhibition of KaiC phosphorylation	-	++
(b)	non-competitive inhibition of KaiC phosphorylation	+	++
(c)	KaiC dephosphorylation	++	++
(d)	KaiA-dependent KaiC dephosphorylation	-	++

Table II-1

The dependency of periodic oscillations on the formulae of phosphorylation functions. The results were obtained by linear stability analysis. I used four types of *Phos* depending on the assumptions made for KaiB's function, and analyzed if oscillations in the Transcriptional Activation Model (TAM) and the Transcriptional Repression Model (TRM) can occur. ++, oscillation can occur; +, oscillation can occur, though the amplitude of P-KaiC is very small in the computer simulation; -, oscillation cannot occur.

effectors	observed effect	TAM	TRM
kaiA$^-$	repress transcription and abort oscillation	++	–
kaiB$^-$	abort oscillation and induce transcription	++	–
kaiC$^-$	repress transcription and abort oscillation	++	–
OX-*kaiA*	induce transcription and abort oscillation	++	–
OX-*kaiA* in *kaiC*$^-$	no effect on *kaiC*$^-$ phenotype	+	–
OX-*kaiC*	repress transcription and abort oscillation	+	++
OX-*kaiC* in *kaiA*$^-$	slightly induce transcription	–	*ND*
OX-nonphosphorylatable *kaiC* mutant	transiently repress and gradually induce transcription	–	–
KaiA activity rate	shorten the period	–	++
KaiB activity rate	lengthen the period	+	++
KaiC degradation rate	lengthen the period	++	++

Table II-2

Summary of the experimentally observed phenotypes, and the results of computer simulation of *kai* mutants, and overexpression studies. *kaiA*$^-$, *kaiA*-inactivated mutant; *kaiB*$^-$, *kaiB*-disrupted mutant; *kaiC*$^-$, *kaiC*-disrupted mutant; OX, overexpression. ++, the phenotype is realized; +, the phenotype is realized depending on the parameter condition; −, the phenotype cannot be realized; ND, not determined; TAM, the Transcriptional Activation Model; TRM, the Transcriptional Repression Model. The effect of OX-*kaiC* in *kaiA*$^-$ in TRM is not determined, because the phenotype of *kaiA*$^-$ cannot be explained in TRM.

Chapter III:
KaiC Phosphorylation Cycle

Introduction

It has been demonstrated that the KaiC phosphorylation cycle persists even under continuous dark conditions when transcription and translation have almost ceased (Tomita *et al.*, 2005). Since cyanobacteria are photosynthetic bacteria, their metabolic rate under dark conditions appears to be lowered severely. Under such conditions, cyanobacteria maintain their clocks using the transcription-less KaiC phosphorylation cycle. The KaiC phosphorylation cycle was reconstituted *in vitro* using a minimal cocktail of three recombinant proteins with ATP. The period of the *in vitro* oscillation is temperature compensated, and the periods observed *in vivo* in KaiC mutant strains were consistent with those measured *in vitro* (Nakajima *et al.*, 2005). These results indicated that KaiC phosphorylation is the molecular timer for the circadian rhythms of cyanobacteria. The *in vitro* oscillator is thus the best available system for providing insight into the molecular mechanisms of the circadian system with chemical resolution.

The striking finding of *in vitro* KaiC phosphorylation cycle confirmed that the interaction between Kai proteins generates the cycle, although the specific mechanism that drives the clock remains unclear. It is reported that KaiC exhibits the periodic interaction with KaiA and KaiB *in vivo* (Fig. III-1) (Kageyama *et al.*, 2003; Kitayama *et al.*, 2003). After phosphorylation, KaiC associates with KaiA, and subsequently with KaiB to form a larger complex. As time progresses, the KaiA-KaiB-KaiC complex dissociates and KaiC is dephosphorylated. These interactions would relate to the regulation of periodic KaiC phosphorylation.

The aim of this chapter is to elucidate the mechanism of the KaiC phosphorylation cycle, where the total amount of KaiC is conserved; however, its status changes periodically. I first present an observation-based model that I call

the basic model. As this model did not show oscillations, I analyzed generalized models and determined conditions of the structure for generating oscillations in a closed system. Based on the theoretical results, I improved the basic model and developed five-variable models, one of which successfully explains the KaiC phosphorylation cycle. I realized the observed pattern of the KaiC phosphorylation cycle and predicted an unknown state that lies between KaiC phosphorylation and the formation of the KaiC/KaiA complex.

Models and Results

Basic model

Based on the possible KaiC behavior proposed by Kitayama *et al*. (Kitayama *et al.*, 2003), I developed a mathematical model for the KaiC phosphorylation cycle *in vitro* (Fig. III-1). KaiC phosphorylation is regulated by KaiA, which is suggested to form two types of complexes; P-KaiC/KaiA and P-KaiC/KaiA/KaiB. With increases in the concentrations of these complexes, the concentration of free KaiA molecules decreases. Based on this fact, I hypothesized that negative feedback from the complex formations to KaiC phosphorylation, which is mediated by the decrease in free KaiA concentration, is responsible for the KaiC phosphorylation cycle. I developed a four-variable model as follows,

$$\begin{aligned}
\frac{dV_1}{dt} &= -\frac{k_{phos} g_1 V_1}{k_m + V_1} + k_{dephos} V_4 \\
\frac{dV_2}{dt} &= \frac{k_{phos} g_1 V_1}{k_m + V_1} - k_{CpA} g_2 V_2 \\
\frac{dV_3}{dt} &= k_{CpA}\, g_2 V_2 - k_{CpAB} h V_3 \\
\frac{dV_4}{dt} &= k_{CpAB} h V_3 - k_{dephos} V_4
\end{aligned} \qquad \text{(III–1a)},$$

$$\begin{aligned}
g_i &= a - [\text{KaiA - containing complex}] - s[\text{P - KaiC/KaiA/KaiB complex}] - a_i \\
h &= b - [\text{P - KaiC/KaiA/KaiB complex}]
\end{aligned} \qquad \text{(III–1b)},$$

where V_1, V_2, V_3, and V_4 are the concentrations of non-phosphorylated KaiC (NP-KaiC), phosphorylated KaiC (P-KaiC), the P-KaiC/KaiA complex, and the P-KaiC/KaiA/KaiB complex, respectively. k_m, k_{phos}, k_{CpA}, k_{CpAB} and k_{dephos} are the

Michaelis constant, the rate for KaiC phosphorylation, the P-KaiC/KaiA complex formation, the P-KaiC/KaiA/KaiB complex formation and dissociation/dephosphorylation, respectively. g_i and h denote the effects of free KaiA and KaiB molecules, respectively. g_1 represents the negative feedback from complex formation to KaiC phosphorylation via KaiA.

~Details of the model and assumptions~

Based on the observation that the KaiC autophosphorylation rate is very low in the absence of KaiA (Williams *et al.*, 2002), I assumed that KaiC phosphorylation requires KaiA and so used the Michaelis-Menten function for this reaction. I assumed that KaiB does not affect KaiC phosphorylation; however, the effect of KaiB on the phosphorylation rate of KaiC is indirectly included via dephosphorylation. Based on the observation that the KaiC dephosphorylation phase and the formation of P-KaiC/KaiA/KaiB start simultaneously (Kitayama *et al.*, 2003), I ignored the rate for dephosphorylation of free P-KaiC (V_2), and assumed that KaiC dephosphorylation occurs simultaneously with the dissociation of the P-KaiC/KaiA/KaiB complex. In this model, an increase of KaiB accelerates the formation of the P-KaiC/KaiA/KaiB complex followed by KaiC dephosphorylation, which negates the phosphorylation rate. At the same time, the effects of KaiA and KaiB on the dephosphorylation rate of KaiC are indirectly included; KaiB does not enhance dephosphorylation in the absence of KaiA in the model. An increase of KaiA decreases KaiC dephosphorylation by accelerating KaiC phosphorylation of NP-KaiC.

To avoid complexity in the model, I did not consider the process of KaiC homohexamer formation and KaiA and KaiB homodimer formations.

The rates of phosphorylation and P-KaiC/KaiA complex formation mediated by free KaiA decreased with the concentration of the KaiA-containing complexes

(V_3 and V_4), and should not be negative. This also applies to the rate of P-KaiC/KaiA/KaiB formation, which decreased with its concentration (V_4). Therefore, I used piecewise defined functions for $g_1(V_3,V_4)$, $g_2(V_3,V_4)$, and $h(V_4)$, respectively,

$$
\begin{aligned}
g_1(V_3,V_4) &= \begin{cases} a - V_3 - sV_4 - a_1 & (a - V_3 - sV_4 - a_1 \geq 0) \\ 0 & (a - V_3 - sV_4 - a_1 < 0) \end{cases} \\
g_2(V_3,V_4) &= \begin{cases} a - V_3 - sV_4 - a_2 & (a - V_3 - sV_4 - a_2 \geq 0) \\ 0 & (a - V_3 - sV_4 - a_2 < 0) \end{cases} \\
h(V_4) &= \begin{cases} b - V_4 & (b - V_4 \geq 0) \\ 0 & (b - V_4 < 0) \end{cases}
\end{aligned}
\qquad \text{(III–2)},
$$

where a and b are the total concentrations for KaiA and KaiB molecules, and a_1 and a_2 are the minimum densities of KaiA required to bring about phosphorylation and complex formation, respectively. s is introduced ($0 < s \leq 1$) to consider the possibility that the number of KaiA molecules may vary in the two types of complexes. g_1, g_2, and h represent negative feedback processes.

~Analyzing the model for instability~

The dynamics of the system were analyzed by focusing on linear stability using the Routh-Hurwitz conditions (see Appendix III-A). From the theory of dynamic systems, the equilibrium surrounded by orbits of cycle needs to be unstable to cause stable cyclic oscillations. I ignored the equilibria that make the values of g_i or h zero in Eq. (III-2), since periodic oscillations around such equilibria are clearly impossible. The system is non-linear, and thus I solved the equilibrium not explicitly but numerically (see Appendix III-B).

After scanning 177,147 parameter sets, the periodic oscillations in KaiC phosphorylation were not realized. This result implied that the model was

inadequate to explain the KaiC phosphorylation cycle.

Generalized models for generic stability conditions

The previous model based on observed facts might not satisfy the necessary conditions of the dynamic structure for showing periodic oscillations in states. To confirm this expectation and to theoretically determine necessary conditions for oscillation, I developed the general frameworks of the dynamic system and analyzed them. In the following general models, I do not indicate the relationship between variables and the states of KaiC proteins.

~Random transition model~

This model includes every possible transition from every state to any other. The transition from state i to state j is denoted by $r_{i\to j}$. Since there is no influx to or outflux from the system, the total amount of the state remains constant. Here, I explain my model using the case when the molecules take five different states (Fig. III-2a). The linearized system around the equilibrium can be written in general as follows,

$$\frac{d}{dt}\begin{pmatrix} V_1 \\ V_2 \\ V_3 \\ V_4 \\ V_5 \end{pmatrix} = \begin{pmatrix} -k_{21}-k_{31}-k_{41}-k_{51} & k_{12} & k_{13} & k_{14} & k_{15} \\ k_{21} & -k_{12}-k_{32}-k_{42}-k_{52} & k_{23} & k_{24} & k_{25} \\ k_{31} & k_{32} & -k_{13}-k_{23}-k_{43}-k_{53} & k_{34} & k_{35} \\ k_{41} & k_{42} & k_{43} & -k_{14}-k_{24}-k_{34}-k_{54} & k_{45} \\ k_{51} & k_{52} & k_{53} & k_{54} & -k_{15}-k_{25}-k_{35}-k_{45} \end{pmatrix}\begin{pmatrix} V_1 \\ V_2 \\ V_3 \\ V_4 \\ V_5 \end{pmatrix} \quad \text{(III–3)},$$

where V_1, V_2, V_3, V_4, and V_5 are concentrations of states 1, 2, 3, 4, and 5, respectively, and k_{ji} is the rate constant of $r_{i\to j}$.. For example, the molecules in state 1 transform into states 2, 3, 4, and 5 at a rate of $k_{21}V_1$, $k_{31}V_1$, $k_{41}V_1$, and $k_{51}V_1$,

respectively. Then, V_1 decreases at a rate of $(-k_{21}-k_{31}-k_{41}-k_{51})V_1$.

If all k_{ij} are positive, the system always holds the stable condition (see Appendix III-A). To destabilize the system, at least one nondiagonal element should be negative. The same result is obtained for systems where the number of variables is lesser or greater (N =3, 4, 5, 6, 7, 8).

The analysis of this general model indicated that to generate a periodic cycle, repressing or promoting interactions are required between the states of this system.

~Closed circuit model~

In this analysis, I identified the condition for generating oscillations in the state transition system. I assumed a closed circuit for the directed transition between states (Fig. III-2b) and considered it to be the basic structure of the dynamics. The linearized dynamics was as follows,

$$\frac{d}{dt}\begin{pmatrix} V_1 \\ V_2 \\ \vdots \\ V_N \end{pmatrix} = \begin{pmatrix} -k_1 & & & k_N \\ k_1 & -k_2 & & \\ & k_2 & \ddots & \\ & & \ddots & -k_N \end{pmatrix}\begin{pmatrix} V_1 \\ V_2 \\ \vdots \\ V_N \end{pmatrix} \quad \text{(III–4)},$$

where V_i is a variable and k_i is the rate constant for $r_{i\to i+1}$,. According to the result obtained from the random transition model, the system was always stable. I added an inhibitory or activating effect to a state transition and examined if such an effect destabilizes the system.

First, I added a single inhibitory path into this system. Let $k_{i,\,j}$ denote the element of ith column and jth row in the transition matrix of Eq. (III-4). Eq. (III-4) can incorporate the inhibition of $r_{i\to i+1}$ by state j, by transforming two elements ($k_{i,\,j} \to k_{i,\,j}-p$, and $k_{i-1,\,j} \to k_{i-1,\,j}+p$). p indicates the intensity of

inhibition by state *j*. The inhibitory effect will produce negative nondiagonal elements in the transition matrix, and may cause instability in the system.

Let us consider an example in the case when $N = 5$. When the reaction $r_{1\to 2}$ is inhibited by state 4, the dynamics are expressed as,

$$\frac{d}{dt}\begin{pmatrix} V_1 \\ V_2 \\ V_3 \\ V_4 \\ V_5 \end{pmatrix} = \begin{pmatrix} -k_1 & 0 & 0 & p & k_5 \\ k_1 & -k_2 & 0 & -p & 0 \\ 0 & k_2 & -k_3 & 0 & 0 \\ 0 & 0 & k_3 & -k_4 & 0 \\ 0 & 0 & 0 & k_4 & -k_5 \end{pmatrix}\begin{pmatrix} V_1 \\ V_2 \\ V_3 \\ V_4 \\ V_5 \end{pmatrix} \qquad \text{(III–5)}.$$

Analysis revealed that this system can become unstable when $p > k_1$. The same result was obtained when either states 5 or 1 inhibited $r_{1\to 2}$, although inhibition by any other state never destabilized the system.

I confirmed this result with a computer simulation using the following formula,

$$\frac{d}{dt}\begin{pmatrix} V_1 \\ V_2 \\ V_3 \\ V_4 \\ V_5 \end{pmatrix} = \begin{pmatrix} -k_1(V_4^*)^{-n} & 0 & 0 & nk_1V_1^*(V_4^*)^{-n-1} & k_5 \\ k_1(V_4^*)^{-n} & -k_2 & 0 & -nk_1V_1^*(V_4^*)^{-n-1} & 0 \\ 0 & k_2 & -k_3 & 0 & 0 \\ 0 & 0 & k_3 & -k_4 & 0 \\ 0 & 0 & 0 & k_4 & -k_5 \end{pmatrix}\begin{pmatrix} V_1 \\ V_2 \\ V_3 \\ V_4 \\ V_5 \end{pmatrix} \qquad \text{(III–6)}.$$

The above formula indicates the special case where $r_{1\to 2}$ is inhibited by state 4. Here, *n* indicates the intensity of the inhibitory effect. The computer simulation (see Appendix III-B) demonstrated that oscillations can be generated from the inhibition caused by states 4 or 5, and not by any other state ($n = 10$, data not shown). When state 1 inhibits $r_{1\to 2}$, the system may become unstable, although

not periodic, for all the parameter sets tested in the computer simulation (data not shown).

I examined all possible inhibitory paths in the cases where N = 3, 4, 5, 6, 7, and 8 (Table III-1). In all cases, the system could be destabilized when the inhibiting state was more than two steps ahead of the inhibited reaction $r_{i\to i+1}$ and the reactant state i (Fig. III-3a). If the inhibiting state was less than three steps ahead from the reactant state, the system was always stable. I call inhibition by a state more than two steps ahead *destabilizing inhibition*, and inhibition by a state within two steps ahead *stabilizing inhibition*. The distance between inhibiting and reactant states does not depend on the system size N.

Next, I assessed the effect of activation. I can incorporate the activation of $r_{i\to i+1}$ by state j, by transforming two elements ($k_{i,j} \to k_{i,j}+p$, and $k_{i-1,j} \to k_{i-1,j}-p$) into the dynamics in Eq. (III-4). It was revealed that the system becomes unstable when $r_{i\to i+1}$ is activated by a state other than the reactant (Fig. III-3b) and $p > k_1$. This result suggested that the activation of state transition was more likely to generate oscillations than inhibition.

Consequently, in the closed circuit model, oscillations occur when the system includes either an inhibition or activation by the state that is far enough from the reactant.

~Multiple inhibition in the closed circuit model~

At present, positive feedback in Kai protein interactions has not been identified. Thus, I focused on the inhibitory effect and confirmed the significance of the relative distances between the recipient reaction and the inhibitor; thereby analyzing the case where more than one state inhibits a transition. I assumed that a series of consecutive states denoted by I, inhibit the reaction $r_{1\to 2}$. The reaction

rate is expressed as,

$$k_1(a - \sum_{I \in j} V_j) \qquad \text{(III-7)},$$

where a is the basal reaction rate in the absence of inhibition. To simplify the analysis, I ignored the dependency of $r_{1\to2}$ on V_1, the reactant concentration. The dynamics of other variables are the same as Eq. (III-4).

Table III-2 shows the results. Among the 16 cases in which I analyzed stability, the system was always stable in 9 and may have become unstable in 7. For the 7 cases, I confirmed the occurrence of oscillations by computer simulations. The results can be intuitively understood based on the idea of *destabilizing inhibition* and *stabilizing inhibition*. The systems that exhibit oscillations possess more *destabilizing inhibitions* than *stabilizing inhibitions*. Meanwhile, stable systems possess more *stabilizing inhibitions* than *destabilizing inhibitions*.

Revised model realizing the KaiC phosphorylation cycle

Let us reconsider the basic model in terms of the concept of *destabilizing inhibition* and *stabilizing inhibition*. Negative feedback from the KaiA-containing complexes to KaiC phosphorylation (g_1) in the basic model was *stabilizing inhibitions* corresponding to the case where V_3 and V_4 inhibited $r_{1\to2}$ in the four-variable system in Table III-2. Other negative feedback processes (g_2 and h) were *stabilizing inhibitions* as well. That is why the basic model never showed periodic oscillations. To realize the KaiC phosphorylation cycle, I increased the distance between the inhibitors and the inhibited transition by assuming a distinct, unknown state between P-KaiC and the P-KaiC/KaiA complex (Fig. III-4). In the revised system, named the five-variable model #1, negative

feedback from the KaiA-containing complexes to KaiC phosphorylation was *destabilizing inhibition*. The dynamics of the model can be expressed as follows,

$$\begin{aligned}
\frac{dV_1}{dt} &= -\frac{k_{phos} g_1 V_1}{k_m + V_1} + k_{dephos} V_4 \\
\frac{dV_2}{dt} &= \frac{k_{phos} g_1 V_1}{k_m + V_1} - k_{new} V_2 \\
\frac{dV_{new}}{dt} &= k_{new} V_2 - k_{CpA} g_2 V_{new} \\
\frac{dV_3}{dt} &= k_{CpA} g_2 V_{new} - k_{CpAB} h V_3 \\
\frac{dV_4}{dt} &= k_{CpAB} h V_3 - k_{dephos} V_4
\end{aligned} \qquad \text{(III-8)},$$

where V_{new} is the concentration of the unknown state and k_{new} is the rate constant for transition from P-KaiC to the unknown state. g_1, g_2, and h are the same functions as in the basic model shown in Eq. (III-2). I also constructed three more systems comprising the five variables shown in Table III-3. The dynamics of the models #2, #3, and #4 are shown in Appendix III-C. In contrast to the five-variable model #1, the five-variable models #2, #3, and #4 contained only *stabilizing inhibitions*.

I examined if these models realized the KaiC phosphorylation cycle by numerical analysis and computer simulation. It was demonstrated that the KaiC phosphorylation cycle occurred only in model #1, as expected. In the other systems, the periodic oscillations in KaiC phosphorylation were not realized after searching 531,441 parameter sets. This result suggested that there should be sufficient length of retardation between the phosphorylation and the complex formation processes.

Fig. III-5a shows the successfully realized pattern of the KaiC phosphorylation cycle. The concentration of each state of KaiC rises and falls periodically (Fig.

III-5b). In this numerical simulation, I chose parameter values for Kai protein concentrations, KaiC phosphorylation, and dephosphorylation rates based on experimental data. In a reconstitution of the KaiC phosphorylation cycle *in vitro* (Nakajima *et al.*, 2005), the concentrations of KaiA, KaiB, and KaiC are estimated at 0.85, 1.31, and 2.35 μM, respectively. Therefore, the concentration of KaiC hexamer was chosen at 400 nM. The stoichiometry of the complex formation of KaiA dimer, KaiB dimer, and KaiC hexamer is unknown. I assumed functional units of KaiA and KaiB at 200 nM. I used the KaiC phosphorylation and dephosphorylation rates at 2.4 /hr and 0.6 /hr, corresponding to 0.66 x 10^{-3} /sec and 0.16 x 10^{-3} /sec, respectively. They are the same order as the estimated values of 10^{-3} to 10^{-4} /sec by Nakajima *et al.* (Nakajima *et al.*, 2005; Tomita *et al.*, 2005).

I also investigated the significance of the unknown state for generating oscillations, by comparing the rate constants for phosphorylation (k_{phos}) and for the transition from P-KaiC to the unknown state (k_{new}). Fig. III-6 shows the conditions for instability, revealing that k_{new} is required not to exceed four times the value of k_{phos} for instability. If the k_{new} value was very large compared to the k_{phos} value, it would become possible to integrate the unknown state into the P-KaiC state. Then, the dynamics would become a four-variable model-like system. The result here showed that retardation of the cyclic dynamics could not be achieved only by delaying the direct transition from P-KaiC to the P-KaiC/KaiA complex. It was also suggested that KaiC-KaiA complex formation required more than one step of posttranslational modification including phosphorylation or conformational change of KaiC.

Discussion

The theoretical conclusion and biological feedback

In this report, I investigated the conditions for realizing the state transition oscillator, where the concentration of each state exhibits oscillations with the total mass of all states remaining constant. From analyses of the generalized models, I demonstrated that at least one state transition process should be inhibited by other states at more than two steps ahead or activated by a state other than the reactant state. Based on the results, I constructed models for the transcription-less KaiC phosphorylation cycle. Using computer simulation, I demonstrated that the KaiC phosphorylation cycle can be generated by two functions of KaiA: enhancing KaiC phosphorylation and forming complexes with KaiC. The complex formation reduces free KaiA molecules, thereby exerting a negative feedback effect toward KaiC phosphorylation. I also predicted that KaiC exists in more than four states, and that an unknown state of KaiC should exist between P-KaiC and the P-KaiC/KaiA complex (Fig. III-4). This result suggested that there should be sufficient length of retardation between the phosphorylation and the complex formation processes. It was also suggested that KaiC-KaiA complex formation requires more than one step of posttranslational modification including phosphorylation or conformational change of KaiC.

In this study, the model did not incorporate positive feedback, though theoretical analysis showed that the condition for generating oscillations by positive feedback was less strict than that by negative feedback. Therefore, other mechanisms for oscillation are also possible. However, if the currently known information on Kai proteins includes most of their essential functions, the results showing that the mechanism responsible for driving the KaiC phosphorylation

cycle is the regulation of KaiC phosphorylation by *destabilizing* negative feedback via KaiA, it seem plausible.

The minimum number of states for oscillation

In a dynamic system of ordinary differential equations, generally a minimum of two variables is required for generating periodic behavior, e.g., Lotka-Volterra equations for prey-predator system (Britton, 2003). In the case of gene expression level systems, the system of a single autoregulatory gene that includes two variables (mRNA and protein) never exhibits stable periodic oscillations. The self-repression system of the gene requires at least three distinct states, such as mRNA, protein, and its phosphorylation for generating oscillations (Goodwin, 1965; Kurosawa *et al.*, 2002). In this study, it was revealed that oscillations driven by the inhibition of state transition require more than four states in a closed state transition system. The conservation law, where the total number of different states is conserved, is considered to be a stricter condition than the formula of gene regulation.

The unknown state

Our results suggested that KaiC-KaiA complex formation requires more than one step of posttranslational modification, including phosphorylation or conformational change of KaiC. In fact, it was observed that accumulation of P-KaiC increases prior to accumulation of the KaiC-KaiA complex (Kitayama *et al.*, 2003). This observation suggested that KaiA does not form a stable complex with KaiC when it is phosphorylated with the aid of KaiA. The theoretical results supported the fact that tight binding of KaiC and KaiA does not occur promptly after KaiC phosphorylation. It is reported that KaiC forms hexamers containing many phosphorylation sites (Mori *et al.*, 2002; Nishiwaki *et al.*, 2004; Xu *et al.*,

2004), and that KaiC is likely to exist in a variety of different combinations of phosphorylation on its various sites (Wang, 2005). These results explained the significance of the multiple phosphorylation states responsible for generating oscillation.

Wang proposed that dimeric KaiA interacts with only two subunits in the KaiC hexamer (Wang, 2005). In this regard, it is suggested that only a few residues on two subunits are phosphorylated at a time. Phosphorylation at a few sites might trigger subsequent phosphorylation in a KaiC hexamer by, for example, conformational changes. This hypothetical event is thus a candidate for the transition of a state to an unknown state or retardation in the computer simulation.

Amplitude of the P-KaiC/KaiA/KaiB complex

In the computer simulation shown in Fig. III-5b, the concentration of the P-KaiC/KaiA/KaiB complex oscillates with a very small amplitude, although it appears to oscillate with a large amplitude in a cell under continuous light conditions (Kageyama *et al.*, 2003; Kitayama *et al.*, 2003). In cells, KaiB is located in both the membrane and cytosol, and is released later from the membrane into the cytosol during late subjective night (Kitayama *et al.*, 2003). This translocation periodically changes the KaiB concentration in the cytosol and may result in the large amplitude of the P-KaiC/KaiA/KaiB accumulation. Indeed, the amplitude of KaiC phosphorylation *in vitro* was not as large as *in vivo*. The amplitude of the concentration of the complex *in vitro* is yet to be examined; however, the computer simulation in this study implied that the amplitude was small *in vitro*.

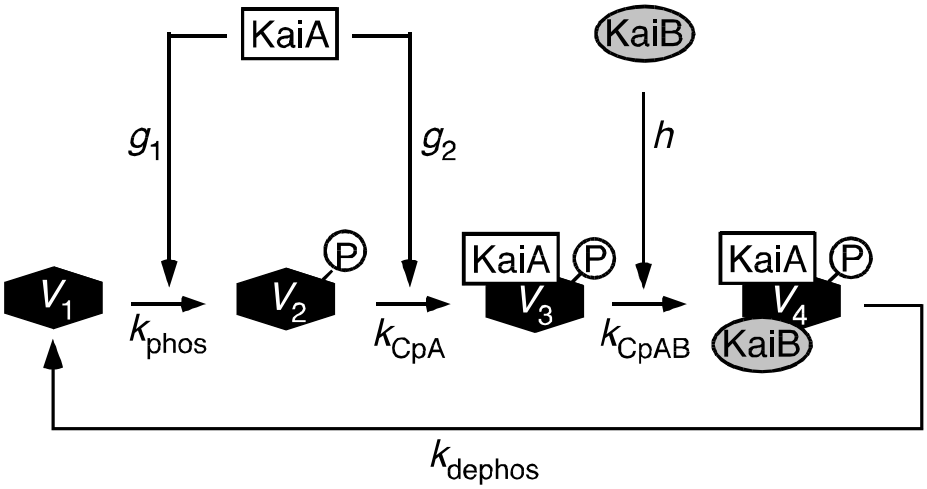

Fig. III-1

The schematic description of the basic model based on the report by Kitayama and colleagues (Kitayama *et al*., 2003). In the early morning, the phosphorylation level of KaiC is relatively low. During the subjective day, the phosphorylated KaiC level gradually accumulates. The P-KaiC/KaiA complex and P-KaiC/KaiA/KaiB accumulate in turn during the late subjective night, and finally the complex dissociates. At the same time, the phosphorylation level of KaiC is reduced. In the basic model, V_1, V_2, V_3, and V_4 denote NP-KaiC, P-KaiC, the P-KaiC/KaiA, and P-KaiC/KaiA/KaiB complexes, respectively. The phosphorylation rate depends on the concentration of free KaiA molecules (designated as g_1) and the rate constant is k_{phos}. The P-KaiC/KaiA complex formation also depends on KaiA (designated as g_2) and the rate constant is k_{CpA}. g_1 and g_2 are reduced with increase of the KaiA-containing complexes. The P-KaiC/KaiA/KaiB complex formation depends on the free KaiB concentration (designated as h) and the rate constant is k_{CpAB}. h is reduced with the increase of the P-KaiC/KaiA/KaiB complex. The rate constant for dissociation of the complex and the KaiC dephosphorylation is designated as k_{dephos}.

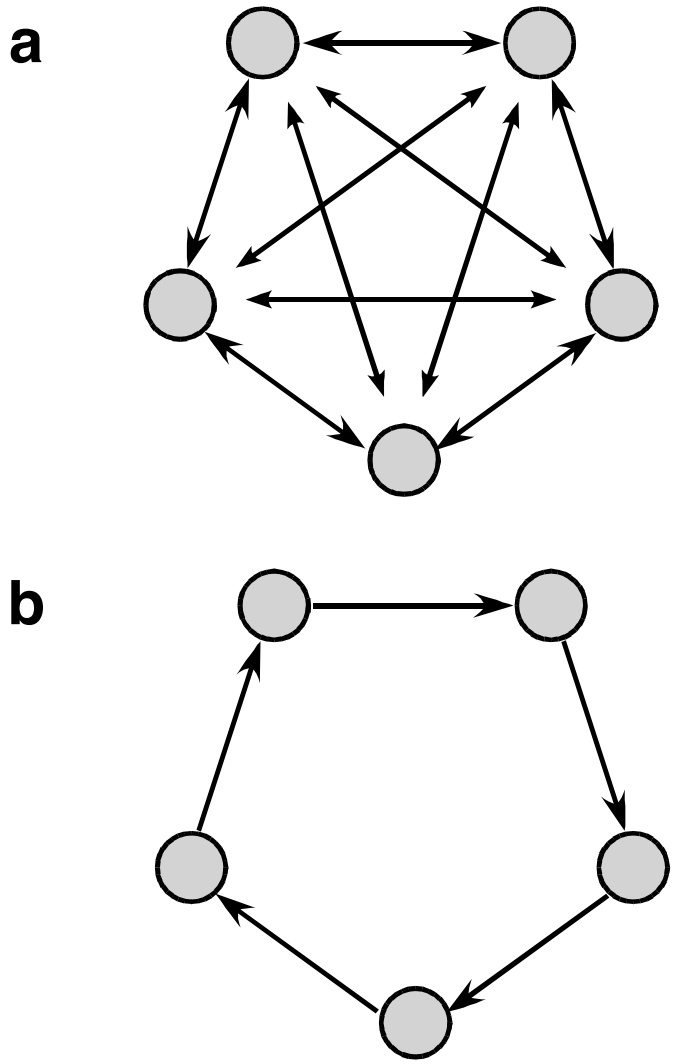

Fig. III-2

Generalized models for state transition in a closed system. These are cases when the system contains five distinct states for each of the oscillating molecules. (a) Random transition model. This general system includes every possible transition from every state to any other state. The circles indicate states of the oscillating molecules and arrows indicate transitions. (b) Closed circuit model. This is a specific form of the random transition model, where the order and direction of transition are determined.

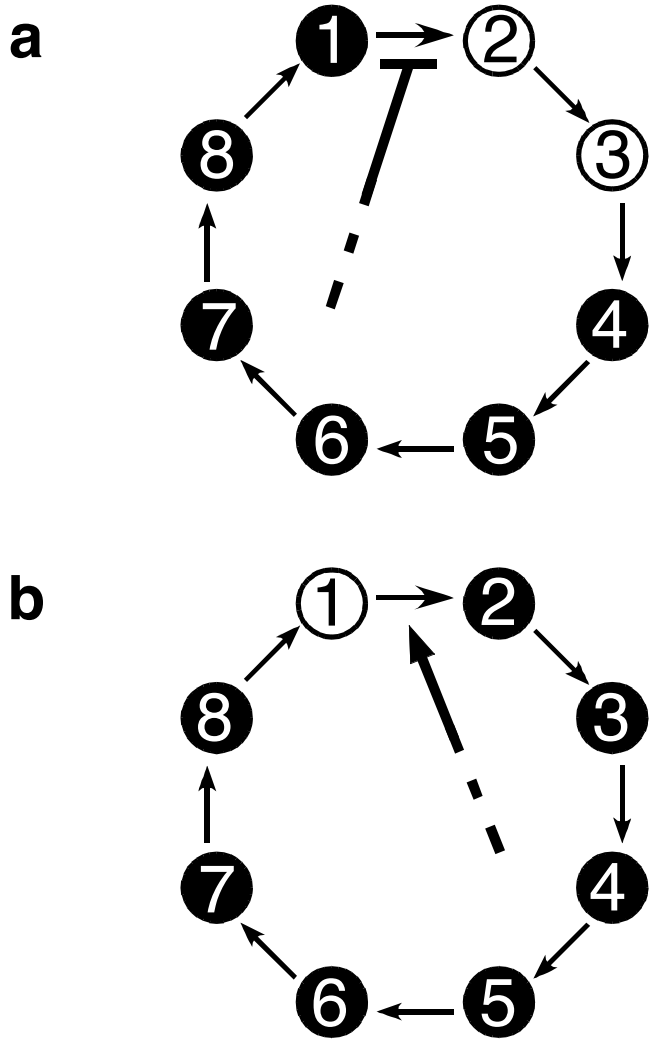

Fig. III-3

The relative distance between the recipient reaction and the effector state that destabilizes the system. These are cases when the system contains eight distinct states for each of the oscillating molecules. (A) Destabilization by inhibition of $r_{1\to 2}$. Closed circles (states 1, 4 - 8) indicate the states that can destabilize the system. Inhibition by the state indicated by open circles (states 2, 3) never destabilizes the system. (B) Destabilization by activation of $r_{1\to 2}$. Closed circles (states 2 - 8) indicate states that can destabilize the system. Activation by the state indicated by open circles (state 1) never destabilizes the system.

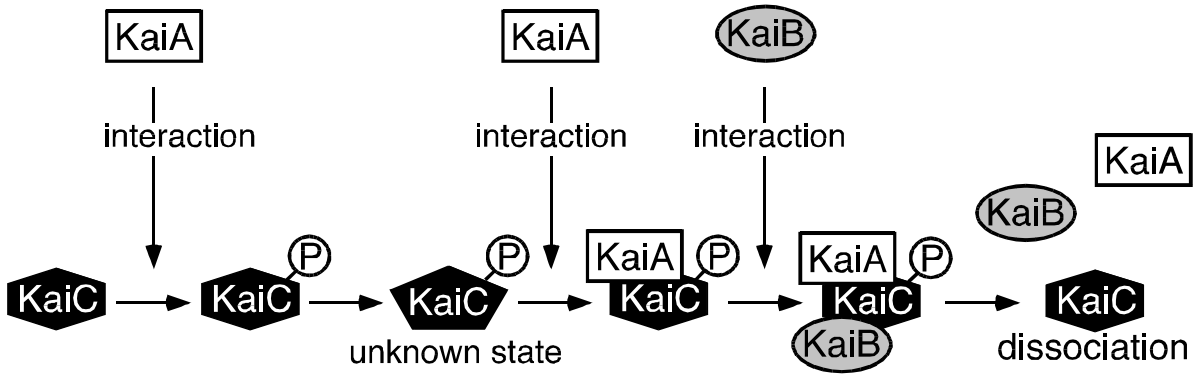

Fig. III-4

The schematic description of the five-variables model #1. This is a possible model for the dynamic regulation of KaiC phosphorylation and Kai protein complex formation. The KaiC phosphorylation rate is regulated by KaiA. P-KaiC is further modified and becomes the unknown state, which might be another phosphorylation status. Accumulation of the unknown state of KaiC accelerates its tight binding to KaiA. The P-KaiC/KaiA complex formation reduces free KaiA molecules, thereby exerting a negative feedback effect toward KaiC phosphorylation. KaiB binds to the stable P-KaiC/KaiA complex and forms the P-KaiC/KaiA/KaiB complex. This final complex formation triggers KaiC dephosphorylation, and dephosphorylated KaiC loses affinity to KaiA and KaiB.

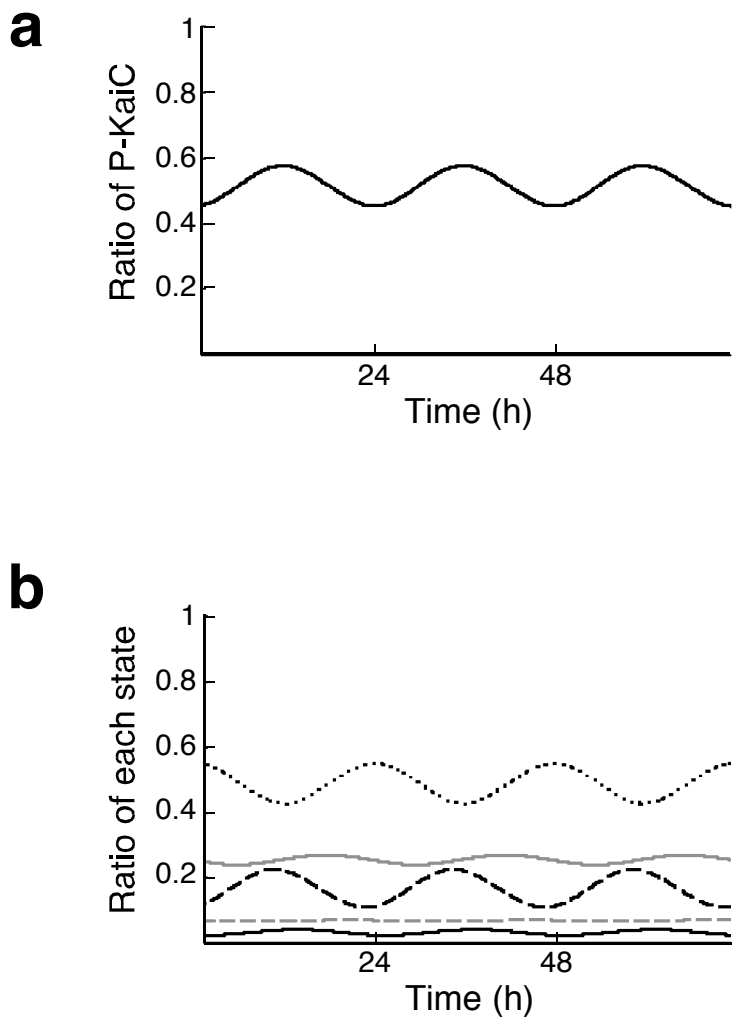

Fig. III-5

Example of temporal changes in the states of KaiC. The horizontal axis represents time. The result was obtained when k_{phos} = 2.4 /hr, k_{new} = 0.24 /hr, k_{CpA} = 0.015 nM/hr, k_{CpAB} = 0.0008 nM/hr, k_{dephos} = 0.6 /hr, k_m = 0.07 nM, a = 200 nM, a_1 = 66 nM, a_2 = 0 nM, b = 200nM, s = 0.8, and ΣV_i = 400 nM. (A) Ratio of P-KaiC to total KaiC. $(V_2 + V_{\text{new}} + V_3 + V_4) / \Sigma V_i$ is plotted. (B) Ratios of non-phosphorylated KaiC (dotted line), phosphorylated KaiC (P-KaiC, black dashed lines), unknown state (black solid line), the P-KaiC/KaiA complex (gray solid line), and the P-KaiC/KaiA/KaiB complex (gray dashed line) to total KaiC.

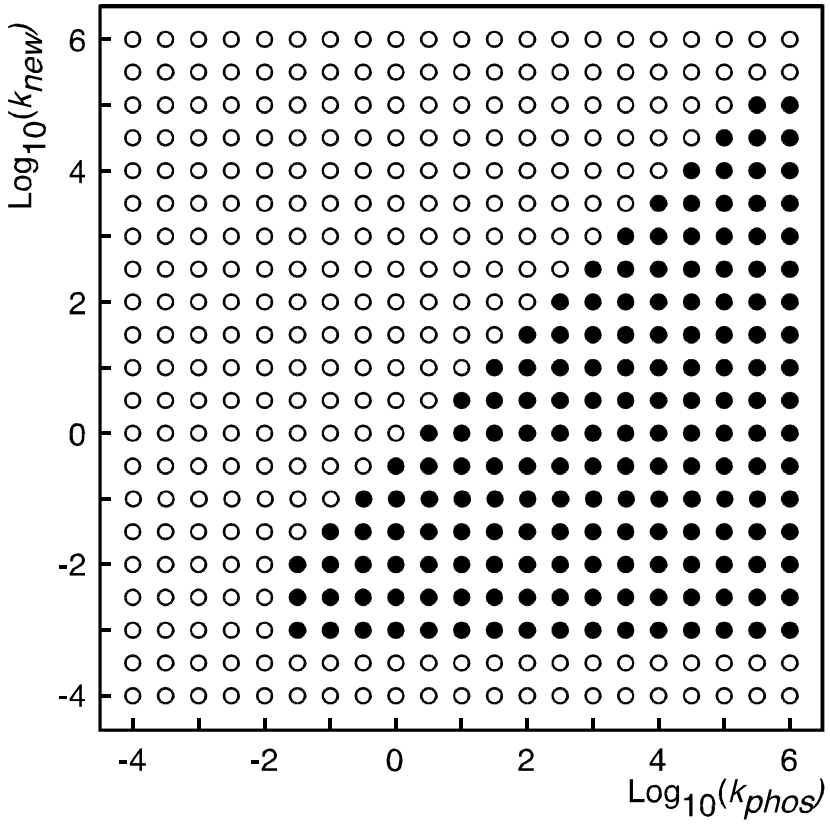

Fig. III-6

The conditions of kphos and knew values for instability. The horizontal and vertical axes are $\log_{10}(k_{phos})$ and $\log_{10}(k_{new})$, respectively. Open circles indicate conditions where the system is stable, and filled circles indicate conditions where instability occurs. The equilibria of the model and the condition for instability are determined by numerically changing parameters: $10^{-2} < k_{phos} < 10^{6}$; $10^{-2} < k_{new} < 10^{6}$; k_{CpA}= 0.00015, 0.015, 1.5 nM/hr; k_{CpAB} = 0.000008, 0.0008, 0.08 nM/hr; k_{dephos} = 0.006, 0.6, 60 /hr; k_m = 0.0007, 0.07, 7 nM. The values of following parameters are fixed: a = 200 nM; a_1 = 66 nM; a_2 = 0 nM; b = 200 nM; s = 0.8; ΣV_i = 400 nM.

number of states in the system	inhibitor							
	V_1	V_2	V_3	V_4	V_5	V_6	V_7	V_8
3	O	×	×	–	–	–	–	–
4	O	×	×	O	–	–	–	–
5	O	×	×	O	O	–	–	–
6	O	×	×	O	O	O	–	–
7	O	×	×	O	O	O	O	–
8	O	×	×	O	O	O	O	O

Table III-1

Destabilization by single inhibition in the closed circuit model. The reaction $r_{1\to2}$ is inhibited by a single state. The stability of the system was determined using the Routh-Hurwitz conditions. ×, the system is always stable; O, can be unstable; –, states that does not exist in the system. The closed circuit model is symmetric for a shift transformation along the circuit pathway.

number of states in the system	inhibitor V_2	V_3	V_4	V_5	V_6	stability
4	•	•		–	–	×
		•	•	–	–	×
5	•	•			–	×
		•	•		–	×
			•	•	–	O
	•	•	•		–	×
		•	•	•	–	O
6	•	•				×
		•	•			×
			•	•		O
				•	•	O
	•	•	•			×
		•	•	•		O
			•	•	•	O
	•	•	•	•		×
		•	•	•	•	O

Table III-2

Destabilization by multiple inhibitions in the closed circuit model. The reaction $r_{1\to 2}$ is inhibited by several inhibitors, as $k_1(a-\sum_{j\in I}V_j)$. •, states included in I ; –, states that do not exist in the system; ×, the system is always stable; O, the system can be unstable.

model	order in the circuit pathway					sustained oscillation
	1	2	3	4	5	
4-val	C	Cp	**CpA**	**CpAB**	−	×
5-val #1	C	Cp	unknown	**CpA**	**CpAB**	O
5-val #2	C	Cp	**CpA**	**unknown**	**CpAB**	×
5-val #3	C	Cp	**CpA**	**CpAB**	**unknown**	×
5-val #4	C	unknown	Cp	**CpA**	**CpAB**	×

Table III-3

Results of numerical analysis and computer simulation in the basic (4-val) and five-variable (5-val) models. C, non-phosphorylated KaiC; Cp, phosphorylated KaiC (P-KaiC); **CpA**, the P-KaiC/KaiA complex; **CpAB**, the P-KaiC/KaiA/KaiB complex; –, a state that does not exist in the system; unknown, the unknown state of KaiC; ×, no oscillatory solutions; O, sustained oscillations were observed in the computer simulation. Bold face, the KaiA-containing complexes, which exert negative feedback effect to KaiC phosphorylation

Chapter IV:
General Discussion

Mathematical models are usually constructed based on experimental facts and incorporate a theoretical vision. In most computational analyses seen today, observed events are simulated using a model composed of many factors, reactions, and finely tuned parameters. However, such methods can only tell that the proposed model is a candidate to mimic known biological behaviors. Therefore, it cannot be assured if the results obtained with the model reflect actual biology. Moreover, the plausibility of such computational strategies and their results naturally depend on the volume of information inputted. It is possible that a model based on a reaction scheme proposed in the past no longer reflects currently updated facts. What I presented in my thesis are novel strategies that can avoid these problems and so predict unknown biological mechanisms ahead of their experimental elucidation.

To begin with, I focused on structural conditions that do not depend on parameter values. I considered that investigating the structure was fundamental, and that considering what can be provided from theoretical studies, this was informative. In fact, in the current stage of Kai oscillator research, not all the chemical reactions between Kai proteins have been identified or examined. Physiological plausibility, therefore, can be properly assessed only for a few parameters. Conversely, in a system where detailed reaction rates can be assessed by experimental results, the part that theoretical studies can play might not have much meaning.

Based on this idea, I adopted two strategies; an exhaustive analysis of a simple framework, and the determination of a regulatory structure, set out in Chapter II and Chapter III, respectively. I abstracted known biological information into a simple structure and identified indispensable interactions between components to generate oscillations. By this method, I

successfully determined the structure of the reaction network of the cyanobacterial circadian system.

For mathematical determinations of the oscillatory conditions, I devised a method based on experimental facts. In the usual understanding of dynamic theories, conditions for oscillations are determined by examining conditions for the presence of limit cycles. However, if an experimental study certified that any initial states will promptly follow the identical orbit of a periodic behavior, it is considered that there is only one stable solution orbit and that the nonlinearity of the dynamic system is not high. The Kai oscillator is largely insensitive to fluctuations of protein concentrations and ratios (Kageyama *et al.*, 2006). In this case, the conditions for the presence of an unstable point at the center of an orbit can be approximately substituted for the conditions for the presence of an oscillation orbit. Therefore, I adopted linear stability analysis, which is a universal method conventionally used to examine instability in the sense that an analysis is applicable to any form of reaction functions. It is expected that in future studies this simple method can be applied to models composed of many variables.

The results in Chapter III included general conditions for oscillations in a closed system. Though the definitions of *stabilizing inhibition* and *destabilizing inhibition* were based on the restraint that the total mass is conserved, this result indicated the general regulative role of negative feedback. Negative feedback may stabilize or destabilize the system depending on the length of the time lag in the feedback. I strictly proved this property mathematically.

An unresolved problem is the cooperation of the two mechanisms of the TTO and non-TTO cycles that are studied in this thesis. The crucial factor is the transcriptional role of phosphorylated KaiC. It has been demonstrated that KaiC phosphorylation is necessary for transcriptional repression activity using an unphosphorylatable KaiC mutant (Nishiwaki *et al.*, 2004). This result is contradictory to the Transcriptional Activation Model, which is seen as being more plausible than the alternative model (Chapter II). In Chapter III, it was predicted that to exert KaiA-mediated *destabilizing inhibition* there should be at least three distinct states for phosphorylated KaiC; an initially phosphorylated state, an unknown state, and the KaiA containing complex. Recent observations reveal that KaiB binds to KaiC before KaiA binds to it *in vitro*, raising the possibility that the unknown state that I predicted corresponds to the KaiB-KaiC complex (Clodong *et al.*, 2007; Kageyama *et al.*, 2006). Further studies on how phosphorylated KaiC changes its role for transcriptional regulation depending on phosphorylation sites or binding statuses remain to be undertaken. The elucidation of this should help determine the phase resetting of the clock, which is indeed one of the major properties defining the circadian clock

The mechanism seen in the most antiquated of organisms indicates the fundamental differences that have arisen in timekeeping mechanisms in the course of evolution. However, it is also considered that the circadian oscillator appears to be generally composed of two coupling loops, the TTO and phosphorylation cycles. Accordingly, it is presumed that, in the course of evolution, clock-evolving organisms chose one of these cycles as

the core loop for their circadian system (Fukada, 2006). For cyanobacteria, photosynthetic organisms where metabolic activity including gene expression is severely lowered in darkness, the low-cost phosphorylation cycle would favorable. Old data also implies a link between photosynthesis and the non-TTO cycle, as photosynthesis in the alga *Acetabularia* can freerun independently of transcription (reviewed in Ditty *et al.*, 2003; Lakin-Thomas and Brody, 2004). Given that the circadian clock and photosynthesis inevitably correlate with the photic signal, the acquisition of the photosynthesis ability possibly was the turning point in the development of the circadian mechanism. This putative evolutionary process implies that phosphorylation also greatly contributes to temperature compensation of the clock in animals.

The *in vitro* reconstitution of the Kai oscillator, a very rare example of a functional biochemical circuit, has motivated many theoretical works. Each model has focused on a distinct aspect of clock dynamics, resulting in a divergence of models of an identical phenomenon. The present models can be categorized into three responsible processes, in accord with the mathematical understandings of those models.

The first mechanism is the “hourglass” circuit for the behavior of the KaiC hexamer. It is assumed that individual hexamers tend to be fully phosphorylated and then fully dephosphorylated in turn (Clodong *et al.*, 2007; Emberly and Wingreen, 2006; van Zon *et al.*, 2007). This phenomenological assumption based on an observation (Kageyama *et al.*, 2006) cannot answer the question of what mechanism allows the appearance of the separation of the phosphorylation- and dephosphorylation-biased phases.

The second is positive feedback, where a state in effect promotes its own production. Especially in a closed system, positive feedback can easily generate oscillations, as I have demonstrated (Chapter III). The regulation by positive feedback is incorporated in models by proposing unidentified function of Kai proteins (Kurosawa *et al.*, 2006; Mehra *et al.*, 2006).

The third is negative feedback. As I proposed (Chapter III), the fact that KaiA binds to phosphorylated KaiC is explained as negative feedback toward phosphorylation by free KaiA depletion (Clodong *et al.*, 2007; Miyoshi *et al.*, 2007). My study is the first to suggest this process, and this type of model supports my results. Miyoshi *et al*. demonstrated simulation-based functional screening and predicted regulation in completely and partially phosphorylated (CP and PP) KaiC promotes and suppresses transcription, respectively (Miyoshi *et al.*, 2007). The difference in transcriptional regulation between CP and PP KaiC enabled simulation of oscillatory behaviors under light and dark conditions, supporting the significance of the unknown state that I predicted (Chapter III) and resolving the discrepancy in the Transcriptional Activation Model (Chapter II). Clodong *et al*. also demonstrated simulation-based screening by using the hourglass design (Clodong *et al.*, 2007). They screened 224 networks involving either positive or negative feedback by reference to robustness, and finally determined just one network with negative feedback via KaiA. Their result strongly supports the notion that the KaiC phosphorylation cycle, as I predicted, relies on negative feedback.

As described, various forms of mathematical models for the Kai oscillator have proposed putative mechanisms mediating circadian oscillations. Among them, my studies, ahead of other theoretical ones,

have successfully determined the essential platform for the Kai clock oscillator. It is expected that experimental studies will verify the propositions, and that mathematical models will interpret new data. This should lead to clearer understandings of the cyanobacterial clock system and its great potential.

Chapter V:
Appendices

Appendix I

Here, I explain the concept of the orthodox model of the molecular mechanism of circadian rhythmicity, recently named a transcription/translation feedback oscillator, or TTO (Lakin-Thomas and Brody, 2004; Tomita *et al.*, 2005).

This model proposes that circadian rhythmicity at the cellular level is driven by rhythmic transcription of clock genes (Fig. V-1). Rhythmic transcription generates rhythmic levels of mRNA, which in turn generates rhythmic levels of clock proteins. Clock proteins negatively feed back on their own transcription to reduce their own expression levels. This negative feedback may occur indirectly through interference with positive elements, that is, proteins that turn on transcription of the clock genes. There are additional complications in the various models, such as posttranslational modifications of clock proteins, requirements for entry of proteins into the nucleus, and several interdependent feedback loops mutually influencing each other. Rhythmic phosphorylation of clock proteins was thought to mediate oscillations, by inducing the destruction of proteins or altering transcriptional activity.

The discovery of the KaiC phosphorylation cycle under transcription-less conditions is the first evidence of the existence of a non-TTO biological rhythm mechanism, and sheds light on the importance of phosphorylation of clock proteins.

Appendix II-A

As described in Mathematical Model, I used the Michaelis-Menten function for KaiA-mediated KaiC autophosphorylation as follows,

$$\frac{k[KaiA]N}{k_m + N} \qquad \text{(II-A-1)}$$

, where [*KaiA*], k_m and k are the KaiA concentration, the Michaelis constant and the phosphorylation rate per KaiA concentration, respectively. It is known that the KaiA level in cells is almost constant throughout the entire circadian cycle (Kitayama *et al.*, 2003). Here, I assumed [*KaiA*] to be constant, and then Eq. (II-4) can be replaced simply as follows,

$$\frac{k_a N}{k_m + N} \quad \text{(II-A-2)}$$

, where k_a is k[*KaiA*] and indicates the maximum phosphorylation rate including KaiA activity.

KaiC has autophosphatase activity, and the dephosphorylation rate can be denoted as $k_d P$, where k_d is the dephosphorylation rate per P-KaiC concentration. When KaiB is not expressed, the total change of phosphorylation and dephosphorylation is as follows,

$$\frac{k_a N}{k_m + N} - k_d P \qquad \text{(II-A-3).}$$

The formula is the basic concept behind my models; however, it does

not include the effect of KaiB. Based on Eq. (II-A-3), I constructed four types of *Phos* function depending on the expected mechanisms of the KaiB function.

(a) KaiB inhibits phosphorylation in a competitive manner

This formula is based on the assumption that KaiB interacts with KaiA. This interaction is expected to decrease the amount of KaiA that can interact with KaiC. Then *Phos* is as follows,

$$Phos = \frac{k_a N}{k_m(1 + k_c'[KaiB]) + V} - k_d P \qquad \text{(II-A-4)}$$

, where k_c' is the efficiency of inhibition per KaiB concentration. As [*KaiB*] is always proportional to the total amount of KaiC, using a constant k_c defined by $k_c = \frac{k_c'[KaiB]}{N + P}$, Eq. (II-A-4) can be written as,

$$Phos = \frac{k_a N}{k_m(1 + k_c(N + P)) + N} - k_d P \qquad \text{(II-A-5)}$$

, where k_c is the KaiB activity rate.

(b) KaiB inhibits phosphorylation in a non-competitive manner

This formula is based on the assumption that KaiB interacts with the KaiA-KaiC intermediate product. I assumed that the interactive binding between KaiB and the intermediate product represses kinase activity. The type (b) *Phos* is as follows,

$$Phos = \frac{k_a N}{k_m + N(1 + k_n'[KaiB])} - k_d P = \frac{k_a N}{k_m + N(1 + k_n(N + P))} - k_d P$$

(II-A-6)

, where k_n' is effect of inhibition per KaiB concentration, and k_n is the product of k_n' and the KaiB/KaiC ratio and indicates KaiB activity.

(c) KaiB enhances dephosphorylation

Here the formula is based on the assumption that KaiB regulates the phosphatase activity of KaiC, as KaiA regulates the kinase activity of KaiC. I assumed that KaiC can dephosphorylated by itself, as in (a) and (b). The type (c) *Phos* is as follows,

$$Phos = \frac{k_a N}{k_m + N} - \frac{k_b'[KaiB]P}{k_{mb} + P} - k_d P = \frac{k_a N}{k_m + N} - \frac{k_b(N + P)P}{k_{mb} + P} - k_d P$$

(II-A-7)

, where k_b' and k_{mb} are the dephosphorylation constant and the Michaelis constant for dephosphorylation, respectively. The constant k_b is the product of k_b' and the KaiB/KaiC ratio and indicates KaiB activity.

(d) KaiB enhances dephosphorylation depending on KaiA

This formula is based on the assumption that KaiC dephosphorylation is accelerated when both KaiA and KaiB interact to KaiC. In this case, I have to consider the competition for KaiA between phosphorylation and dephosphorylation. The total amount of KaiA satisfies,

$$[KaiA] = [KaiAf] + [KaiAC] + [KaiABC] \qquad \text{(II-A-8)}$$

, where [*KaiAf*], [*KaiAC*] and [*KaiABC*] are the concentrations of free KaiA molecules, KaiA-KaiC intermediate product in phosphorylation, and the KaiA-KaiB-KaiC intermediates product in dephosphorylation, respectively. Phosphorylation and dephosphorylation occur in proportion to [*KaiAC*] and [*KaiABC*], respectively. Assuming spontaneous dephosphorylation also occurs in proportion to P-KaiC, *Phos* is as follows,

$$Phos = k_1'[KaiAC] - k_2'[KaiABC] - k_d P \qquad \text{(II-A-9)}$$

, where k_1' and k_2' are the rate constants for phosphorylation and for dephosphorylation, respectively. Using the quasi-steady-state hypothesis, the concentrations of the intermediates can be written using stability constants k_3' and k_4' as follows,

$$\begin{aligned} [KaiAC] &= k_3'[KaiAf]N \\ [KaiABC] &= k_4'[KaiAf][KaiBf]P \end{aligned} \qquad \text{(II-A-10)}$$

, where [*KaiBf*] is the concentration of the free KaiB molecules. It is known that KaiB is abundant comparing to KaiA and KaiC, so I assumed that [*KaiBf*] equals the total amount of KaiB. Substituting Eqs. (II-A-8) and (II-A-9) for Eq. (II-A-10), the type (d) *Phos* was obtained,

$$Phos = \frac{(k_1'k_3'N - k_2'k_4'[KaiB]P)[KaiA]}{1 + k_3'Vn + k_4'[KaiB]P} - k_d P = \frac{k_1 N - k_2(N+P)P}{1 + k_3 N + k_4(N+P)P} - k_d P \qquad \text{(II-A-11)}$$

, where k_1, k_2, k_3 and k_4 are constants. The parameter k_1 is the maximum phosphorylation rate including KaiA activity, k_2 is the maximum dephosphorylation rate including KaiA and KaiB activities, k_3 is the stability constant for phosphorylation, and k_4 is the stability constant for dephosphorylation including KaiB activity.

This function corresponds with a simplified reaction scheme based on the fact that KaiC forms complexes with KaiA and KaiB (Kageyama *et al.*, 2003).

Appendix II-B

Basically, I investigated the conditions needed for gene regulation to generate oscillation by numerical methods, where the equilibrium value and stability were determined based on given parameters. However, in cases where type (b) *Phos* or the simplified formula of (c) *Phos* was used, it was possible to obtain an equilibrium of the dynamics though it was not in explicit but an implicit form. Here I explain the latter case. An analysis in the case of type (b) *Phos* is possible by a similar method.

From Eq. (II-1), I assume that there is an equilibrium (U^*, N^* ,P^*) satisfying the following,

$$\begin{aligned} U^* &= \frac{F(N^*,P^*)}{q_u} \\ pU^* - Phos(N^*,P^*) - q_n N^* &= 0 \\ Phos(N^*,P^*) - q_p P^* &= 0 \end{aligned} \quad . \qquad \text{(II-B-1)}$$

Now I introduce μ, satisfying $\mu = pU^*$. By giving a fixed value for μ, N^* and P^* can be formally determined using the second and third equations in Eq. (II-B-1). Assuming that in type (c) *Phos*, k_m and k_{mb} are very small and q_n=q_p=q, equilibria can be obtained as follows,

$$\begin{aligned} N^* &= \frac{\mu(k_d+q)-(k_a q - k_b \mu)}{q(k_d+q)} \\ P^* &= \frac{k_a q - k_b \mu}{q(k_d+q)} \end{aligned} \quad . \text{(II-B-2)}$$

The above assumption may not be appropriate when I search for the conditions for the Transcriptional Repression Model. In that case, a numerical method should be used for determining the stability condition. Using the first equation of Eq. (II-B-1) and the determined form of N^* and P^*, U^* is also determined as a function of N^*, P^* and μ. The Jacobian matrix of the model is as follows,

$$\begin{pmatrix} -1 & \lambda U^*(U^*-1)\cos\theta & \lambda U^*(U^*-1)sin\theta \\ \mu/U^* & k_b - q & k_b + k_d \\ 0 & -k_b & -(k_b+k_d)-q \end{pmatrix} \quad \text{(II-B-3).}$$

The characteristic equation of three-dimensional dynamics in the general form is as follows,

$$x^3 + a_1x^2 + a_2x + a_3 = 0 \qquad \text{(II-B-4)}$$

, where the roots x are the eigenvalues, and the coefficients a_1, a_2 and a_3 of this model are as follows;

$$\begin{aligned} a_1 &= k_d + 2q + 1 \\ a_2 &= q(k_d+q) + k_d + 2q + \mu\lambda(1-U^*)\cos\theta \\ a_3 &= q(k_d+q) + (k_d+q+k_2)\mu\lambda(1-U^*)\cos\theta - k_2\mu\lambda(1-U^*)sin\theta \end{aligned}$$
(II-B-5)

The condition for Hopf bifurcation is that Eq. (II-B-5) has roots of a pair of complex conjugates and that the real part of the roots go from negative to positive. Assuming the other negative real root is α, the cubic equation Eq. (II-B-5) is written as,

$$(x-\alpha)\left(x^2+(a_1+\alpha)x+\alpha^2+\alpha a_1+a_2\right)=0 \qquad \text{(II-B-6)}$$

, where α, is the following,

$$\alpha=\frac{\sqrt[3]{2}r}{3s}-\frac{r}{3\sqrt[3]{2}}-\frac{k_d+2q+1}{3}$$

$$r=-k_d(k_d+q-1)-(q-1)^2+3\mu\lambda(1-U^*)\cos\theta$$
$$s=\sqrt[3]{t+\sqrt{4r^3+t^2}}$$
$$t=(2k_d+q-1)(k_d+2q-2)(k_d-q+1)-9\mu\lambda(1-U^*)(3k_2 sin\theta-(2k_d+q-1+3k_2)\cos\theta)$$
(II-B-7).

Now the condition for the Hopf bifurcation is as follows,

$$\begin{aligned}&\alpha<0\\&\alpha+a_1>0\\&-3\alpha^2+2\alpha a_1+{a_1}^2-4a_2<0\end{aligned} \qquad \text{(II-B-8).}$$

These inequalities can be written in terms of parameters using Eqs. (II-B-5) and (II-B-7). By substituting parameter values (including μ), I numerically determined the instability condition of the equilibrium based on Hopf bifurcation. The parameter μ ($= pU^*$) includes U^*. However, I interpret the numerical change of μ as the change of p in the analysis.

Appendix III-A

Here, I show the analytical form for the random transition model when the system contains four distinct states. The dynamics and characteristic polynomial are as follows,

$$\frac{d}{dt}\begin{pmatrix} V_1 \\ V_2 \\ V_3 \\ V_4 \end{pmatrix} = \begin{pmatrix} -a-b-c & d & g & j \\ a & -d-e-f & h & k \\ b & e & -g-h-i & l \\ c & f & i & -j-k-l \end{pmatrix}\begin{pmatrix} V_1 \\ V_2 \\ V_3 \\ V_4 \end{pmatrix}$$

$$\lambda^4 + A_1\lambda^3 + A_2\lambda^2 + A_3\lambda + A_4 = 0 \qquad \text{(III-A-1)},$$

where a~l are the rate constants of the transitions and λ_i is the eigenvalue. The model here maintains $A_4 = 0$ since the sum of the variables $\sum_i V_i$ is conserved. $A_N = 0$ for any system of N variables in the closed system. In Eq. (III-A-1), the Routh-Hurwitz conditions for stability are expressed as follows (Murray, 1989a),

$$\begin{aligned} &A_1 > 0, \\ &A_3 > 0, \\ &A_1A_2 - A_3 > 0, \end{aligned} \qquad \text{(III-A-2)}.$$

A_1, A_2 and A_3 for Eqs. (III-A-1) and (III-A-2) are given as,

$$A_1 = a+b+c+d+e+f+g+h+i+j+k+l$$
$$A_2 = (a+b+c)(d+e+f)+(g+h+i)(j+k+l)+(a+b+c+d+e+f)(h+i+j)$$
$$+ g(a+c+d+e+f)+k(a+b+c+d+e)+l(b+f)$$
$$A_3 = (a+b+c)(d+e+f)(h+i+j+l)+(a+c+d+e+f)(g+h+i)(j+k+l)$$
$$+ b(h+i)(j+k+l)+f(j+l)(g+h+i)+g(a+c)(d+e+f)+k(d+e)(a+b+c)$$
$$A_1A_2 - A_3 = (a+b+c+d+e+f+g+h+i+j+k+l)(a+c+d+e)(g+h+i+j+k+l)$$
$$+ b(a+b+c+d+e+f+g+h+i+j+k+l)(h+i+j+k+l)$$
$$+ f(a+b+c+d+e+f+g+h+i+j+k+l)(g+h+i+j+l)$$
$$+ (a+b+c+d+e+f+)(a+b+c)(d+e+f)$$
$$+ (g+h+i+j+k+l)(g+h+i)(j+k+l)$$

(III-A-3).

When all a~l are positive, the right hand side of Eq. (III-A-3) contains only positive terms. Thus, A_1, A_2, A_3, and $A_1A_2-A_3$ are always positive, indicating that the system is always stable and V_1, V_2, V_3, and V_4 will converge to equilibrium.

In the same way, I can show the stability of higher dimensional systems.

Appendix III-B

Analysis for instability

The equilibria of the model were determined numerically. The condition for instability of each equilibrium was then examined based on Appendix III-A. These procedures were done by Mathematica (Wolfram) changing all parameters: k_{phos} = 0.024, 2.4, 240 /hr; k_{CpA} = 0.00015, 0.015, 1.5 nM/hr; k_{CpAB} = 0.000008, 0.0008, 0.08 nM/hr; k_{dephos} = 0.006, 0.6, 60 /hr; k_m = 0.0007, 0.07, 7 nM; a = 2, 200, 20000 nM; a_1 = 0, a/3, a/10 nM; a_2 = 0, a/3, a/10 nM; b = 2, 200, 20000 nM; s = 0.04, 0.2, 1; $V_1+V_2+V_3+V_4$ = 4, 400, 40000 nM (in the basic model); k_{new} = 0.0024, 0.24, 24 /hr; $V_1+V_2+V_3+V_4+V_{new}$ = 4, 400, 40000 nM (in the five-variable models). I scanned 3^{11} = 177,147 and 3^{12} = 531,441 parameter sets in the basic and five-variable models, respectively.

In the basic model, and the five-variable models #2, #3, and #4, the equilibria of the system were not determined numerically in 328, 54, 629, and 670 sets, respectively, and the other cases satisfy the condition for stability. For the cases in which equilibria were not determined, I confirmed by computer simulation that the dynamics do not generate oscillations.

In the five-variable model #1, 33,577 sets do not satisfy the stability condition. They are candidates for showing periodic oscillations. I sampled some of them and confirmed that these parameter sets show oscillations of state transition in a computer simulation.

Computer simulation

In a computer simulation, I used the simple explicit difference method

with $\Delta t = 0.0000001$ for the basic model, closed circuit model, and five-variable models. I calculated the changes in the concentrations of each state with time. The computer program was written in C and was calculated on a Linux operating system.

Appendix III-C

In the five-variable models, the property of the unknown state was assigned according to its position in the circuit pathway (Table III-3). The dynamics of the models #2 (Eq. (III-C-1)), #3 (Eq. (III-C-2)), and #4 (Eq. (III-C-3)) are as follows,

$$\begin{aligned}
\frac{dV_1}{dt} &= -\frac{k_{phos}g_1V_1}{k_m+V_1} && + k_{dephos}V_4 \\
\frac{dV_2}{dt} &= \frac{k_{phos}g_1V_1}{k_m+V_1} - k_{CpA}g_2V_2 \\
\frac{dV_3}{dt} &= k_{CpA}g_2V_2 - k_{new}V_3 \\
\frac{dV_{new}}{dt} &= k_{new}V_3 - k_{CpAB}hV_{new} \\
\frac{dV_4}{dt} &= k_{CpAB}hV_{new} - k_{dephos}V_4
\end{aligned} \qquad \text{(III-C-1a)},$$

$$g_i = \begin{cases} a-(V_3+V_{new})-sV_4-a_i & (a-(V_3+V_{new})-sV_4-a_i \geq 0) \\ 0 & (a-(V_3+V_{new})-sV_4-a_i < 0) \end{cases}$$

(III-C-1b)

$$\begin{aligned}
\frac{dV_1}{dt} &= -\frac{k_{phos}g_1V_1}{k_m+V_1} && + k_{dephos}V_{new} \\
\frac{dV_2}{dt} &= \frac{k_{phos}g_1V_1}{k_m+V_1} - k_{CpA}g_2V_2 \\
\frac{dV_3}{dt} &= k_{CpA}g_2V_2 - k_{CpAB}hV_3 \\
\frac{dV_4}{dt} &= k_{CpAB}hV_3 - k_{new}V_4 \\
\frac{dV_{new}}{dt} &= k_{new}V_4 - k_{dephos}V_{new}
\end{aligned} \qquad \text{(III-C-2a)},$$

$$g_i = \begin{cases} a - V_3 - s(V_{new} + V_4) - a_i & (a - V_3 - s(V_4 + V_{new}) - a_i \geq 0) \\ 0 & (a - V_3 - s(V_4 + V_{new}) - a_i < 0) \end{cases}$$

$$h = \begin{cases} b - (V_{new} + V_4) & (b - (V_4 + V_{new}) \geq 0) \\ 0 & (b - (V_4 + V_{new}) > 0) \end{cases}$$

(III-C-2b),

$$\begin{aligned} \frac{dV_1}{dt} &= -k_{new} V_1 & & & k_{dephos} V_4 \\ \frac{dV_{new}}{dt} &= k_{new} V_1 - \frac{k_{phos} g_1 V_{new}}{k_m + V_{new}} & & & \\ \frac{dV_2}{dt} &= & \frac{k_{phos} g_1 V_{new}}{k_m + V_{new}} - k_{CpA} g_2 V_2 & & \\ \frac{dV_3}{dt} &= & & k_{CpA} g_2 V_2 - k_{CpAB} h V_3 & \\ \frac{dV_4}{dt} &= & & & k_{CpAB} h V_3 - k_{dephos} V_4 \end{aligned}$$

(III-C-3).

h in the model #2, and g_i and h in the model #4 are the same as in the model #1 shown in Eq. (III-2).

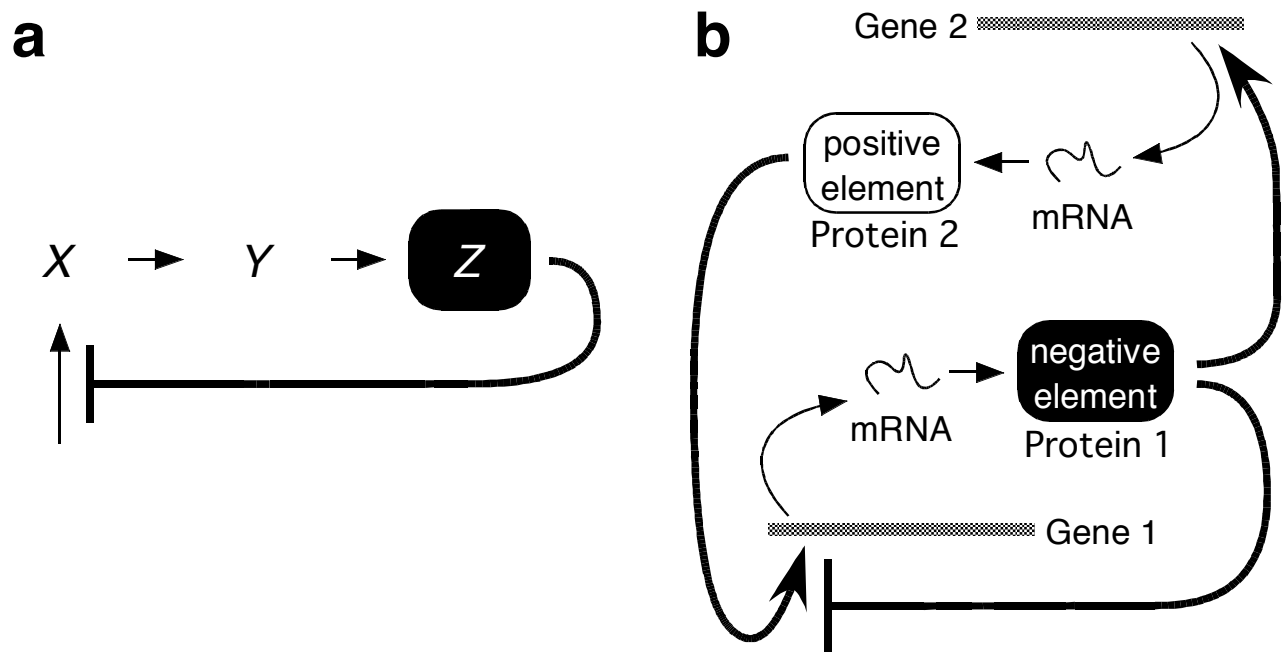

Fig. V-1

Oscillatory networks. Biosynthetic pathways are shown as thin lines with arrowheads. Positive and negative influences are shown as heavy lines with large arrowheads and crossbars, respectively. (a) The mathematical model of oscillatory behavior in enzymatic control processes (Goodwin, 1965). It is assumed that *Z,* produced from *Y,* inhibits production of *X* that produces *Y.* It was demonstrated that this minimal network can generate sustaining oscillation. The variables here can be interpreted as mRNA (*X*), protein in cytoplasm (*Y*), and protein in nucleus (*Z*). (b) The generic model of transcription-translation feedback oscillator (TTO) for circadian clocks. Clock genes are transcribed into mRNA and translated into proteins, which are positive and negative elements. Here, protein 2 positively regulates the transcription of Gene 1. Protein 1 negatively regulates its own transcription by interfering with the positive effect of Protein 2. Protein 1 also positively regulates the production of Protein 2. The positive loop via the positive element contributes to increasing the amplitude. Positive and negative elements are CYC/CLK and PER/TIM in *Drosophila*, CLOCK/BMAL1 and PER/CRY in mammal, FRQ and WC-1/WC-2 in *Neurospora*, respectively.

Chapter VI:
References

Allada R (2003) Circadian clocks: a tale of two feedback loops. *Cell* **112**:284-286.

Britton NF (2003) Population dynamics of interacting species. In *Essential Mathematical Biology*, NF Britton, ed, pp 47–81, Springer, London.

Clodong S, Duhring U, Kronk L, Wilde A, Axmann I, Herzel H and Kollmann M (2007) Functioning and robustness of a bacterial circadian clock. *Molecular systems biology* **3**:90.

Ditty JL, Williams SB and Golden SS (2003) A cyanobacterial circadian timing mechanism. *Annual review of genetics* **37**:513-543.

Dunlap JC (1999) Molecular bases for circadian clocks. *Cell* **96**:271-290.

Emberly E and Wingreen NS (2006) Hourglass model for a protein-based circadian oscillator. *Phys Rev Lett* **96**:038303.

Foster R and Kreitzman L (2004) Rhythms of Life, Profile Books Ltd., London.

Fukada Y (2006) Molecular approach to the circadian clock systems. *Jikken Igaku* **24**:446-451.

Glossop NR, Lyons LC and Hardin PE (1999) Interlocked feedback loops within the *Drosophila* circadian oscillator. *Science* **286**:766-768.

Goldbeter A (1995) A model for circadian oscillations in the *Drosophila* period protein (PER). *Proc Biol Sci* **261**:319-324.

Goldbeter A (2002) Computational approaches to cellular rhythms. *Nature* **420**:238-245.

Goodwin BC (1965) Oscillatory behavior in enzymatic control processes. *Adv Enzyme Regul* **3**:425-438.

Hardin PE (2006) Essential and expendable features of the circadian timekeeping mechanism. *Current opinion in neurobiology* **16**:686-692.

Hardin PE, Hall JC and Rosbash M (1990) Feedback of the *Drosophila* period gene product on circadian cycling of its messenger RNA levels. *Nature* **343**:536-540.

Imai K, Nishiwaki T, Kondo T and Iwasaki H (2004) Circadian rhythms in the synthesis and degradation of a master clock protein KaiC in cyanobacteria. *J Biol Chem* **279**:36534-36539.

Ishiura M, Kutsuna S, Aoki S, Iwasaki H, Andersson CR, Tanabe A, Golden SS, Johnson CH and Kondo T (1998) Expression of a gene cluster *kaiABC* as a circadian feedback process in cyanobacteria. *Science* **281**:1519-1523.

Iwasaki H, Nishiwaki T, Kitayama Y, Nakajima M and Kondo T (2002) KaiA-stimulated KaiC phosphorylation in circadian timing loops in cyanobacteria. *Proc Natl Acad Sci U S A* **99**:15788-15793.

Kageyama H, Kondo T and Iwasaki H (2003) Circadian formation of clock protein complexes by KaiA, KaiB, KaiC, and SasA in cyanobacteria. *J Biol Chem* **278**:2388-2395.

Kageyama H, Nishiwaki T, Nakajima M, Iwasaki H, Oyama T and Kondo T (2006) Cyanobacterial circadian pacemaker: Kai protein complex dynamics in the KaiC phosphorylation cycle *in vitro*. *Mol Cell* **23**:161-171.

Keener J and Sneyd J (1998) The Hodgkin-Huxley model. In *Mathematical Physiology*, pp 129-150, Springer, New York.

Kitayama Y, Iwasaki H, Nishiwaki T and Kondo T (2003) KaiB functions as an attenuator of KaiC phosphorylation in the cyanobacterial circadian clock system. *Embo J* **22**:2127-2134.

Kondo T, Mori T, Lebedeva NV, Aoki S, Ishiura M and Golden SS (1997) Circadian rhythms in rapidly dividing cyanobacteria. *Science* **275**:224-227.

Kondo T, Strayer C, Kulkarni R, Taylor W, Ishiura M, Golden S and Johnson C (1993) Circadian rhythms in prokaryotes: luciferase as a reporter of circadian gene expression in cyanobacteria. *Proc Natl Acad Sci U S A* **90**:5672-5676.

Kurosawa G, Aihara K and Iwasa Y (2006) A model for the circadian rhythm of cyanobacteria that maintains oscillation without gene expression. *Biophys J* **91**:2015-2023.

Kurosawa G, Mochizuki A and Iwasa Y (2002) Comparative study of circadian clock models, in search of processes promoting oscillation. *J Theor Biol* **216**:193-208.

Lakin-Thomas PL and Brody S (2004) Circadian rhythms in microorganisms: new complexities. *Annu Rev Microbiol* **58**:489-519.

Mehra A, Hong CI, Shi M, Loros JJ, Dunlap JC and Ruoff P (2006) Circadian rhythmicity by autocatalysis. *PLoS Comput Biol* **2**:e96.

Miyoshi F, Nakayama Y, Kaizu K, Iwasaki H and Tomita M (2007) A mathematical model for the Kai-protein-based chemical oscillator and clock gene expression rhythms in cyanobacteria. *J Biol Rhythms* **22**:69-80.

Mochizuki A (2005) An analytical study of the number of steady states in gene regulatory networks. *J Theor Biol* **(null)**:(null).

Mori T, Binder B and Johnson C (1996) Circadian gating of cell division in cyanobacteria growing with average doubling times of less than 24 hours. *Proc Natl Acad Sci U S A* **93**:10183-10188.

Mori T, Saveliev SV, Xu Y, Stafford WF, Cox MM, Inman RB and Johnson CH (2002) Circadian clock protein KaiC forms ATP-dependent hexameric rings and binds DNA. *Proc Natl Acad Sci U S A* **99**:17203-17208.

Murray JD (1989a) Appendix B. Routh-Hurwitz Conditions, Jury Conditions, Descartes' Rule of Signs and Exact Solutions of a Cubic. In *Mathematical Biology*, SS Antman, JE Marsden, L Sirovich and S Wiggins, eds, pp 507–509, Springer, Heidelberg.

Murray JD (1989b) Models for Interacting Populations. In *Mathematical Biology*, SS Antman, JE Marsden, L Sirovich and S Wiggins, eds, pp 79-118, Springer, Heidelberg.

Nakahira Y, Katayama M, Miyashita H, Kutsuna S, Iwasaki H, Oyama T and Kondo T (2004) Global gene repression by KaiC as a master process of prokaryotic circadian system. *Proc Natl Acad Sci U S A* **101**:881-885.

Nakajima M, Imai K, Ito H, Nishiwaki T, Murayama Y, Iwasaki H, Oyama T and Kondo T (2005) Reconstitution of circadian oscillation of cyanobacterial KaiC phosphorylation in vitro. *Science* **308**:414-415.

Nishiwaki T, Iwasaki H, Ishiura M and Kondo T (2000) Nucleotide binding and autophosphorylation of the clock protein KaiC as a circadian timing process of cyanobacteria. *Proc Natl Acad Sci U S A* **97**:495-499.

Nishiwaki T, Satomi Y, Nakajima M, Lee C, Kiyohara R, Kageyama H, Kitayama Y, Temamoto M, Yamaguchi A, Hijikata A, Go M, Iwasaki H, Takao T and Kondo T (2004) Role of KaiC phosphorylation in the circadian clock system of *Synechococcus elongatus* PCC 7942. *Proc Natl Acad Sci U S A* **101**:13927-13932.

Preitner N, Damiola F, Lopez-Molina L, Zakany J, Duboule D, Albrecht U and Schibler U (2002) The orphan nuclear receptor REV-ERBalpha controls circadian transcription within the positive limb of the mammalian circadian oscillator. *Cell* **110**:251-260.

Tomita J, Nakajima M, Kondo T and Iwasaki H (2005) No transcription-translation feedback in circadian rhythm of KaiC phosphorylation. *Science* **307**:251-254.

van Zon JS, Lubensky DK, Altena PR and ten Wolde PR (2007) An allosteric model of circadian KaiC phosphorylation. *Proc Natl Acad Sci U S A* **104**:7420-7425.

Wang J (2005) Recent cyanobacterial Kai protein structures suggest a rotary clock. *Structure (Camb)* **13**:735-741.

Wijnen H and Young MW (2006) Interplay of circadian clocks and metabolic rhythms. *Annual review of genetics* **40**:409-448.

Williams SB, Vakonakis I, Golden SS and LiWang AC (2002) Structure and function from the circadian clock protein KaiA of *Synechococcus elongatus*: a potential clock input mechanism. *Proc Natl Acad Sci U S A* **99**:15357-15362.

Woelfle MA, Ouyang Y, Phanvijhitsiri K and Johnson CH (2004) The adaptive value of circadian clocks: an experimental assessment in cyanobacteria. *Curr Biol* **14**:1481-1486.

Xu Y, Mori T and Johnson CH (2003) Cyanobacterial circadian clockwork: roles of KaiA, KaiB and the *kaiBC* promoter in regulating KaiC. *Embo J* **22**:2117-2126.

Xu Y, Mori T, Pattanayek R, Pattanayek S, Egli M and Johnson CH (2004) Identification of key phosphorylation sites in the circadian clock protein KaiC by crystallographic and mutagenetic analyses. *Proc Natl Acad Sci U S A* **101**:13933-13938.

Young MW and Kay SA (2001) Time zones: a comparative genetics of circadian clocks. *Nat Rev Genet* **2**:702-715.

Acknowledgements

I am deeply indebted to my supervisor, Associate Professor Atsushi Mochizuki, for his guidance and stimulating suggestions during the time of my research and in the writing of this thesis. The opportunity he gave me to work on this research project has been an invaluable learning process for me.

I appreciate the insightful comments Professor Takao Kondo has given me. I am also grateful to Associate Professor Hideo Iwasaki for giving me the opportunity to be involved in research related to the cyanobacterial clock. I am likewise obliged to Tokitaka Oyama, Hiroshi Ito, Taeko Nishiwaki, and Masato Kageyama for offering suggestions for improvement of the models and for sharing unpublished data.

I also thank all members of the lab for their help and valuable advice.

As my previous experience in molecular biology underpinned my completion of this thesis, I am full of gratitude to Prof. Kunio Shiota at the University of Tokyo, Dr. Kiyoshi Takayama at Taisho Pharmaceutical Co., Ltd., and Prof. Fumihiko Matsuda at the Centre National de Génotypage.

For this research, I was financially supported by the Research Fellowship for Young Scientists from the Japan Society for the Promotion of Science. As well, I owe the realization of my research life to the National Institutes for Natural Sciences, for improving the environment for scientists with children.

I would like to give special thanks to my husband, Takuya Imamura, who through his close support and encouragement in every situation enabled me to complete this work.

This thesis is dedicated to our daughter.